The Role of a Polar/Subtropical Jet Superposition in the May 2010 Nashville Flood

Andrew C. Winters and Jonathan E. Martin *

Department of Atmospheric and Oceanic Sciences, University of Wisconsin-Madison, Madison, Wisconsin, USA

* *Corresponding author address:* Jonathan E. Martin, Department of Atmospheric and Oceanic Sciences, University of Wisconsin-Madison, 1225 W. Dayton St., Madison, WI 53706.

E-mail: jemarti1@wisc.edu

ABSTRACT

Contributions to the increased poleward moisture flux that characterized the second day of the May 1-3 Nashville Flood of 2010 are examined from the perspective of polar and subtropical jet superposition and its influence on the secondary ageostrophic circulation. Employing the Sawyer-Eliassen circulation equation, the analysis reveals that the poleward moisture flux attributed to the jet increased nearly 120% prior to the second day of the event in response to the superposed jet's ageostrophic circulation, helping to further fuel the production of heavy rainfall.

The full Sawyer-Eliassen circulation associated with the superposed jet is further partitioned into its geostrophic and diabatic components. The geostrophic forcing drove middle tropospheric ascent that fueled the production of deep convection and the record rainfall. The diabatic component, through forcing lower tropospheric ascent and vigorous lower tropospheric poleward moisture flux, provided the link between the tropical moisture and the deep convective environment. Since superposed jets, by their nature, develop on the poleward edge of the tropical or subtropical air, it is suggested that such a mutually reinforcing interaction between these two component forcings of the secondary circulation may routinely characterize the involvement of superposed jet structures in high impact weather events.

1. Introduction

During the first two days of May 2010, two consecutive mesoscale convective systems (MCSs) were responsible for historic rainfall accumulations in excess of 180 mm (7 in.) over a large portion of Tennessee, southern Kentucky, and northern Mississippi (Fig. 1). A few locations saw significantly higher rainfall totals, according to the National Weather Service office in Nashville, with Camden, Tennessee tallying 493 mm (19.41 in.) and Nashville recording 344 mm (13.54 in.) during that two-day period. In addition to the heavy rainfall, both days were characterized by tornado outbreaks, as the environment was weakly stratified and favorable for severe convective development. This combination of sensible weather had enormous and wide-ranging impacts across the entire region, closing numerous roads, resulting in 26 flood related fatalities, causing around $2 billion in property damage in the greater Nashville area, and swelling area rivers to record crests. Specifically, the Cumberland River at Nashville recorded a crest of 15.8 m (51.9 ft), which was 1.3 m (4.3 ft) higher than the previous record at the station in the post flood control era (National Weather Service 2011; hereafter NWS 2011).

One of the most notable aspects of this event, as diagnosed in the work of Moore et al. (2012, hereafter M12), was the presence of an anomalous and narrow plume of enhanced water vapor transport, or an atmospheric river (Newell et al. 1992 and Zhu and Newell 1998), that extended from the Gulf of Mexico northward into the eastern United States. While several recent studies have investigated the impacts of atmospheric rivers on orographically-forced precipitation events (e.g. Ralph et al. 2006; Stohl et al. 2008; Guan et al. 2010), the M12 study demonstrated that atmospheric rivers can also play a considerable role in heavy rainfall events that are synoptically forced, such as those that occur over the central and eastern United States.

Specifically, M12 found that a southerly low-level jet, driven by a strong geopotential height gradient between a lee trough along the east coast of Mexico and a strong subtropical ridge north of the Caribbean Sea, facilitated much of the anomalous moisture transport out of Central America and into the southern Mississippi River Valley. Furthermore, they noted that this moisture transport strengthened over the northern Gulf of Mexico and southern Mississippi River Valley in the hours preceding the second day of the event (their Fig. 6). This finding was also noted in subsequent studies of the Nashville flood (Durkee et al. 2012; Lackmann 2013; Lynch and Schumacher 2013). These studies have demonstrated that this persistent and increased moisture transport into the region over the two-day period, in conjunction with ascent along stationary, convectively generated outflow boundaries, aided in the production of heavy rainfall across portions of Tennessee, Kentucky, and northern Mississippi.

Coincident with the increase in moisture transport prior to the second day of heavy rainfall, however, was a relatively rare vertical superposition of the normally distinct polar and subtropical jet streams and an attendant acceleration of jet wind speeds (see M12, their Fig. 4). Observational analysis by Defant and Taba (1957, hereafter DT57) of tropopause temperature (their Fig. 3) demonstrates that, in such a superposition, the upper tropospheric and lower stratospheric baroclinicity associated with each jet is intensified. As a result, a superposed jet structure possesses an anomalous fraction of the pole-to-equator temperature gradient (manifest as available potential energy (APE)). This suggests that much stronger upper tropospheric and lower stratospheric fronts and an anomalously deep layer of vertical shear, as required by the increased horizontal baroclinicity, accompany the relatively rare superposition of the polar and subtropical jets.

The development of intensified frontal structure associated with the superposed jet is often attended by a strengthening of its transverse, ageostrophic secondary circulation, diagnosable using the Sawyer-Eliassen circulation equation (Sawyer 1956; Eliassen 1962). Such ageostrophic circulations have been shown in numerous studies to play an important role in the production of sensible weather. For example, much attention has been focused on upper tropospheric fronts, which can form as a result of the differential vertical motions associated with Sawyer-Eliassen circulations and are an important part of the extratropical cyclone life cycle (e.g. Uccellini et al. 1985; Whitaker et al. 1988; Barnes and Colman 1993; Lackmann et al. 1997). Additionally, the circulations associated with upper tropospheric fronts have been shown to play an important role in the development of convective precipitation events, as first suggested by Omoto (1965) and further demonstrated by Hobbs et al. (1990) and Martin et al. (1993). While a number of studies have qualitatively considered the moisture flux accomplished by the lower tropospheric horizontal branches of ageostrophic jet circulations (e.g. Uccellini and Johnson 1979; Uccellini et al. 1984; Uccellini and Kocin 1987), direct quantification of these effects has not received as much attention in the literature. Furthermore, if the static stability is low in a given region, as it was over the southern Mississippi River Valley on 1-2 May 2010, a Sawyer-Eliassen circulation can occupy a considerable depth of the troposphere. In such a situation, the horizontal winds associated with the secondary circulation near the surface are capable of significant contributions to the moisture transport into the region.

While M12 and Durkee et al. (2012) acknowledge a strengthening of both the jet and moisture flux prior to the second day of heavy rainfall, they do not investigate the link between these processes. Consequently, the modulation of the structure and intensity of the Sawyer-Eliassen circulation by the diabatic residue of the heavy rainfall that characterized this event remains to be considered. In order to address these issues, the present study aims to 1) quantify the contribution to the poleward moisture flux made by the superposed jet's ageostrophic circulation and 2) examine the impact that both geostrophic and diabatic forcing may have had in determining the strength and sense of the overall ageostrophic circulation.

The remainder of this study is organized as follows. Section 2 gives an overview of the methodology used to identify superposed jets as well as background on the Sawyer-Eliassen circulation equation. Section 3 provides a brief synoptic overview of the flooding event. Section 4 discusses the impacts of the Sawyer-Eliassen circulations during each day of the event and further dissects the forcing responsible for the superposed jet's ageostrophic circulation. Finally, Section 5 presents a discussion and conclusions.

2. Methodology

This study is performed using model analyses from the National Centers for Environmental Prediction (NCEP) Global Forecast System (GFS) at 6-h intervals with a horizontal grid spacing of 1.0° × 1.0° and a vertical grid spacing of 50 hPa (25 hPa between 1000 hPa and 900 hPa). In order to accommodate the identification scheme that follows, these data were bi-linearly interpolated onto isentropic surfaces at 5K intervals from 300K to 370K using programs within the General Meteorology Package (GEMPAK) (desJardins et al. 1991).

a. Jet Identification

The work by DT57 identified the characteristic three-step pole-to-equator tropopause structure shown in Fig. 2 (modified from their Fig. 13), wherein each step is separated from its neighbors by the presence of a westerly wind maximum. They found that, on average, the tropical tropopause[1] was found at around 90 hPa (17-18 km) and extended to 30°N, roughly the poleward edge of the Hadley Cell. Near that latitude the tropopause height abruptly lowers to about 200 hPa (12 km), with the subtropical jet nestled within that break in the tropopause (e.g. Loewe and Radok 1950; Yeh 1950; Koteswaram 1953; Mohri 1953; Koteswaram and Parthasarathy 1954; Sutcliffe and Bannon 1954; Krishnamurti 1961; Riehl 1962). Poleward of this feature was what DT57 termed the "middle tropopause" located around 250 hPa. The polar jet is found in the break between the middle tropopause and the even lower polar tropopause (300 hPa) near 50°N. While relatively modest baroclinicity in the upper troposphere and lower stratosphere characterizes the subtropical jet, the polar jet

[1]DT57 identified the tropopause via analysis of soundings. The tropopause was identified at the elevation of "a noticeable change of tropospheric lapse rate to an isothermal layer or to an increase of temperature with height." p. 261, DT57.

sits atop the strongly baroclinic, tropospheric-deep polar front (e.g. Namias and Clapp 1949; Palmén and Newton 1948; Newton 1954; Palmén and Newton 1969; Keyser and Shapiro 1986; Shapiro and Keyser 1990).

The DT57 analysis also demonstrated the utility of maps of tropopause height (in hPa) for locating the position of the jets. On these maps, one of which is shown in Fig. 3 (modified from DT57 Fig. 2), DT57 referred to sharp, isolated, and easily identifiable gradients of tropopause height as “breaklines”. These breaklines were found to be coincident with the respective jet maxima (e.g. the subtropical jet is found at the breakline between the tropical and middle tropopause). While such an analysis demonstrates that these jets typically occupy different latitude bands, substantial meanders in the jets are common. Additionally, the characteristic latitudinal separation between the two structures occasionally disappears, as it does in Fig. 3 south of Iceland over the North Atlantic, where the polar and subtropical jets vertically superpose. These observations of the tropopause structure, both climatologically and instantaneously, form the theoretical basis for the following jet identification scheme.

The identification scheme for the polar, subtropical, and superposed jet streams is described with reference to the features illustrated in Fig. 4. Figure 4a depicts an example of clearly separate polar and subtropical jets in the eastern North Pacific. A vertical cross section through these distinct features unambiguously identifies the separate jet cores (Fig. 4b). From this cross section, it is clear that the core of the polar jet, located at approximately 300 hPa, is largely contained within the 315-330K isentropic layer while the subtropical jet core, located at approximately 200 hPa, occupies the 340-355K layer. Additionally, both the polar and the subtropical jets lie at the low potential vorticity (PV) edge of the strong horizontal PV gradient that separates the upper troposphere from the lower stratosphere in their respective layers. With these attributes in mind, the identification scheme evaluates characteristics of the PV and wind speed distributions in each grid column of analysis data. Within the 315-330K (340-355K) layer, whenever the magnitude of the PV gradient within the 1-3 PVU channel exceeds an empirically determined threshold value[2] *and* the integrated wind speed in the 400-100 hPa layer exceeds 30 m s^{-1}, a polar (subtropical) jet is identified in that grid column. The occurrence of both polar and subtropical jet characteristics in a single grid column identifies a jet superposition event at that time in that grid column. An example of a jet superposition event is shown in a plan view in Fig. 4c. Not until a vertical slice through the jet core is examined can the superposition be identified (Fig. 4d). Notice that, rather than the three-step tropopause structure identified by DT57 and shown in Fig. 4b, a superposed jet is characterized by a two-step tropopause structure with a steep tropopause wall from the polar to the tropical tropopause. This nearly vertical PV wall (from roughly 550 hPa to 150 hPa in this case) is the leading structural characteristic of a superposed jet.

b. Sawyer-Eliassen Circulation Equation

A particularly useful way to interrogate the vertical circulations associated with jet-front structures, in nearly straight flow, is afforded by the Sawyer-Eliassen circulation equation (Sawyer 1956; Eliassen 1962):

$$(-\gamma\frac{\partial\theta}{\partial p})\frac{\partial^2\psi}{\partial y^2} + (2\frac{\partial M}{\partial p})\frac{\partial^2\psi}{\partial p\partial y} + (-\frac{\partial M}{\partial y})\frac{\partial^2\psi}{\partial^2 p} = Q_g - \gamma\frac{\partial}{\partial y}(\frac{d\theta}{dt}) \tag{1}$$

where γ is a constant on isobaric surfaces ($\gamma = (R/fp_0)(p_0/p)^{c_v/c_p}$), $p_0 = 1000$ hPa, $c_v = 718$ J kg^{-1} K^{-1}, $c_p = 1004$ J kg^{-1} K^{-1}, R is the gas constant for dry air, θ is the potential temperature, and f is the Coriolis parameter. M is the absolute geostrophic momentum ($M = U_g - fy$) and U_g and V_g are the along- and across-front geostrophic winds, respectively. Q_g is the geostrophic forcing term, which is the sum of the shearing ($Q_{SH} = 2\gamma[(\partial U_g/\partial y)(\partial\theta/\partial x)]$) and stretching deformation terms ($Q_{ST} = 2\gamma[(\partial V_g/\partial y)(\partial\theta/\partial x)]$). The ageostrophic circulation lies in a plane transverse to the frontal boundary (jet axis) and is determined by the

[2]The threshold values are 1.4×10^{-5} PVU m^{-1} (1.4×10^{-11} m K kg^{-1} s^{-1}) for the 315-330K layer and 0.9×10^{-5} PVU m^{-1} for the 340-355K layer.

Sawyer-Eliassen streamfunction, ψ, such that $v_{ag} = -\partial\psi/\partial p$ and $\omega = dp/dt = \partial\psi/\partial y$. Given the second-order nature of this differential equation, positive (negative) values for the forcing function correspond to negative (positive) values for the streamfunction and thermally direct (indirect) circulations. The coefficients of the second-order terms on the left hand side of (1) represent the static stability, baroclinicity, and inertial stability, respectively. For the full derivation and discussion of (1), the reader is referred to Eliassen (1962) or Keyser and Shapiro (1986).

From (1), it becomes evident that knowledge of the distribution of U_g, V_g, M, θ, and $d\theta/dt$, in a particular case, allows for the calculation of the coefficients on the left hand side of (1) as well as the forcing function. Consequently, absolute temperature and geostrophic wind are extracted from each grid point in the GFS analysis at 50 hPa vertical intervals from 1000 hPa to 50 hPa. These variables are then interpolated onto the selected vertical cross section perpendicular to the jet axis. Subsequently, all of the coefficients and geostrophic forcing terms in (1) are calculated from these interpolated variables at each grid point within the interior of the cross section. Model vertical motion and relative humidity data are also extracted from the GFS analysis and interpolated onto the cross sectional grid in order to determine $d\theta/dt$, or the rate of latent heating. Following the method of Emanuel et al. (1987), this term is calculated as:

$$\frac{d\theta}{dt} = \omega\left(\frac{\partial\theta}{\partial p} - \frac{\Gamma_m}{\Gamma_d}\frac{\theta}{\theta_e}\frac{\partial\theta_e}{\partial p}\right) \tag{2}$$

where ω is the model vertical motion, θ_e is the equivalent potential temperature, and Γ_m and Γ_d are the moist and dry adiabatic lapse rates, respectively. θ_e is determined using the Bolton (1980) approximation for the Clausius-Clapeyron relationship and the method of Bryan (2008), which contains assumptions that are particularly accurate in heavily precipitating situations.

Once all coefficients and forcing have been determined, successive over-relaxation (SOR) is used to converge on a solution for the Sawyer-Eliassen streamfunction. Since (1) is a second-order elliptic differential equation, a unique solution is guaranteed only when the quasi-geostrophic potential vorticity (QGPV) is greater than zero at each grid point. Therefore, in order to facilitate convergence, if any grid point has QGPV less than zero, the SOR algorithm calculates a 4-point average of the Sawyer-Eliassen streamfunction at the neighboring grid points and assigns the averaged value to the grid point of interest during each iteration. For the solutions[3] presented here, the ageostrophic streamfunction is set to zero on the boundaries of the cross section, as in the solutions presented by Todsen (1964) and Shapiro (1981).

Employing (1), Shapiro (1982) demonstrated that, in the absence of along-jet geostrophic temperature advection, the ageostrophic circulations associated with geostrophic stretching deformation resembled the traditional four-quadrant model with a thermally direct (indirect) circulation in the jet entrance (exit) region (Fig. 5a). Along-jet geostrophic temperature advection mobilizes the geostrophic shearing deformation forcing, which 'shifts' the thermally direct (indirect) circulation to the anticyclonic (cyclonic) shear side of the jet for cases of geostrophic cold air advection, such that subsidence is present through the jet core (Fig. 5b). Conversely, geostrophic warm air advection along the jet acts to 'shift' the thermally direct (indirect) circulation to the cyclonic (anticyclonic) shear side of the jet such that ascent occurs through the jet core (Fig. 5c)[4]. These vertical motions have been shown by numerous studies to exert a considerable influence on restructuring the tropopause and baroclinicity in the upper troposphere and lower stratosphere (e.g. Reed and Sanders 1953; Reed 1955; Shapiro 1981; Shapiro 1982; Keyser and Pecnick 1985; Lang and Martin 2012) and can affect the production of sensible weather.

[3]Inspection of the computed ageostrophic circulation in cross sections immediately upstream and downstream of those selected for the forthcoming analysis were extremely consistent.

[4]These circulations can also be understood in terms of positive/negative vorticity advection by the thermal wind (i.e. Sutcliffe 1947) as described by Martin (2014).

3. The 1-2 May 2010 Nashville Flood - Overview

M12 and Durkee et al. (2012) provide excellent overviews of the meso- and synoptic-scale processes responsible for the production of precipitation across the region and the reader is referred to those works for any additional details. Here, we present an abbreviated synoptic overview of the period from 0000 UTC 1 May - 0000 UTC 2 May across the contiguous United States.

Figure 6 illustrates the anomalous nature of the moisture that was in place during the week of the event and shows that most of the region east of the Mississippi River was characterized by precipitable water values that were at least 5 mm greater than normal for late April/early May. The figure also captures the filamentary structure of the anomaly pattern over the Gulf of Mexico, typical of an atmospheric river. Furthermore, Nashville observed a precipitable water value of 51.3 mm (2.02 in.) at 0000 UTC 2 May, registering well above the 99th percentile for that time of year (45.7 mm) and indicating an almost unprecedented availability of moisture in the troposphere throughout the duration of the flooding event (NWS 2011).

The large-scale pattern at 0000 UTC 1 May (Fig. 7a) depicted an occluding mid-latitude cyclone, with a sea-level pressure (SLP) minimum below 988 hPa, located along the North Dakota/Manitoba border. A warm front at the surface extended across the northern Great Lakes eastward towards New York, while a cold front stretched from northeastern Minnesota southward into eastern Texas. Immediately to the east of the cold front was a tongue of poleward moisture flux at 925 hPa, which flowed from the Gulf of Mexico into the Great Lakes. Maximum poleward moisture flux values[5] over the northern Gulf of Mexico were greater than 30 cm s^{-1} at this time along the axis of maximum moisture flux [6]. At 250 hPa,

[5]Poleward moisture flux is computed as the product of the y-direction velocity, v (m s^{-1}), and the mixing ratio (kg kg^{-1}). Given typical values for mixing ratio (5 g kg^{-1}) and wind speed (10 m s^{-1}), this calculation would yield a moisture flux of .05 m s^{-1} or 5 cm s^{-1}.

[6]Defined as the axis of maximum convergence of the moisture flux gradient vector, it is included as a common reference point for determining the impact of the forthcoming Sawyer-Eliassen circulations on the

a polar jet, as denoted by the blue arrow, stretched from Baja California northeastward into the Central Plains in association with a deep upper-level trough over the western United States, while a subtropical jet, as identified by the red arrow, extended across northern Mexico and eastward along the Gulf Coast. At this time, note that even though the two jets were in relatively close proximity to one another, they were not superposed.

By 0000 UTC 2 May (Fig. 7b), the mid-latitude cyclone had remained stationary along the Canadian border and had begun to decay. The cold front, while making slight progress to the east over the Great Lakes, was stationary over portions of the southern Mississippi River Valley, helping to focus precipitation over the same areas for a second consecutive day. Notably, the poleward moisture flux at 925 hPa was substantially larger than at the earlier time, with maximum values over the northern Gulf of Mexico now exceeding 40 cm s^{-1} along the axis of maximum moisture flux. Coincident with this increase in moisture flux was the first indication of a jet superposition in the upper troposphere over portions of southwestern Oklahoma and western Texas, as denoted by the purple line. This jet superposition was characterized by a rapid acceleration of the jet core wind speeds, which exceeded 70 m s^{-1} at this time.

A cross section along the line C-C' in Fig. 7b, perpendicular to the jet core, is shown in Fig. 8 and confirms the presence of a superposed jet. Rather than the three-step tropopause structure described by DT57, this cross section is characterized by a two-step tropopause structure with a vertical PV wall that distinguishes the break between the polar (400 hPa) and the tropical tropopause (125 hPa). Also note that the identification criteria for the polar and the subtropical jet are both met within the same vertical grid column that intersects the jet core. The superposed jet is also associated with considerable upper tropospheric and lower stratospheric baroclinicity, as required to support the increased vertical wind shear. The coincidence of the observed increase in poleward moisture flux with a proximate jet superposition event suggests that the ageostrophic circulation associated with the superposed

poleward moisture flux.

jet may have played a role in the increased poleward moisture flux observed over the southern Mississippi River Valley.

To investigate this possibility, Fig 9a depicts the total change in the 925 hPa poleward moisture flux across the southern Mississippi River Valley during the 24-h period from 0000 UTC 1 May - 0000 UTC 2 May. Results demonstrate that the poleward moisture flux increases by roughly 9 cm s^{-1} south of the Gulf Coast in the vicinity of the axis of maximum moisture flux at both times. This is in general agreement with the qualitative assessment made from Fig. 7. However, an examination of the difference in the geostrophic poleward moisture flux over the same period (Fig. 9b) shows little to no change along the axes of maximum moisture flux. Instead, increased geostrophic fluxes are displaced to the north and east, consistent with a shift of the strongest southerly geostrophic winds in that direction. So, while M12 and Durkee et al. (2012) note that the largest fraction of the moisture flux was accomplished by geostrophic processes during this event, the majority of the observed *increase* in moisture flux south of New Orleans is accounted for by changes in the ageostrophic poleward moisture flux (which includes the effects of the jet circulation, as well as curvature, friction, etc). Figure 9c confirms this notion, depicting an increase on the order of 9 cm s^{-1} along the Gulf Coast and centered squarely on the axes of maximum moisture flux. Given this conclusion, the analysis that follows aims to determine the specific impact of the superposed jet circulation on the ageostrophic moisture flux over the northern Gulf of Mexico.

4. Diagnosis of Sawyer-Eliassen Circulations

The analysis begins with an investigation of the role the ageostrophic circulation associated with the superposed jet played in facilitating poleward moisture flux into the southern Mississippi River Valley. The individual forcing terms for the superposed jet circulation are then examined to better understand their impacts on the resultant circulation.

a. *Role of Superposed Jet in Facilitating Poleward Moisture Flux*

At 0000 UTC 1 May, an area of convection was beginning to form over portions of central Arkansas. These thunderstorms would later move off to the east and form the first MCS that dropped considerable rainfall amounts across portions of the Tennessee River Valley on the first day of the event. Additionally, the polar and subtropical jets bifurcated over northern Texas, with the polar jet extending to the northeast over the Central Plains while the subtropical jet stretched eastward along the Gulf Coast (Fig. 7a). As such, a diagnosis at this time must consider the separate ageostrophic circulations associated with each jet and its overall contribution to the poleward moisture flux across the southern Mississippi River Valley.

Figure 10a shows the Sawyer-Eliassen circulation along the cross section from D-D' in Fig. 7a, which is cut through the subtropical jet's exit region and is nearly parallel to the axis of maximum moisture flux near the Gulf Coast. The solution depicts a rather weak thermally indirect circulation with the strongest upward vertical motions and streamfunction maximum centered close to Little Rock, Arkansas (LZK), largely associated with the diabatic effects of the ongoing convection (not shown). Over the northern Gulf of Mexico, where the poleward moisture flux was maximized at this time, the role of the Sawyer-Eliassen circulation is rather unimpressive, with a maximum contribution on the order of 5 cm s^{-1} around 925 hPa. A comparison with the total observed ageostrophic poleward moisture flux at this time (Fig. 10b) shows that the magnitude of the poleward moisture flux associated with the Sawyer-Eliassen circulation is on par with observed ageostrophic flux values over the northern Gulf of Mexico. As a result, it is reasonable to conclude that our calculation accurately captures the maximum contribution to the overall moisture flux made by the subtropical jet's ageostrophic circulation in that region.

As previously indicated, the polar jet was located further to the north and west over the Central Plains. Figure 11 demonstrates that the Sawyer-Eliassen circulation associated with the polar jet, along the cross-section E-E' in Fig. 7a, is a stronger, thermally *direct* circulation, such that the low-level, horizontal branch of this circulation actually opposes the poleward moisture flux promoted by the subtropical jet. However, the juxtaposition of these two circulations is favorable for promoting upward vertical motions directly over Little Rock, where the ascending branches of both circulations are collocated. Therefore, while the separate jet circulations likely played a symbiotic role in aiding the initial formation of convection that occurred over central Arkansas at 0000 UTC 1 May, the subtropical jet's circulation was the only one capable of facilitating a poleward moisture flux into the southern Mississippi River Valley at that time.

At 0000 UTC 2 May, an area of convection was ongoing over portions of southern Arkansas and northern Louisiana. As mentioned previously (and illustrated in Fig. 7), the poleward moisture flux increased considerably over the intervening 24-h to a maximum value greater than 40 cm s^{-1}, coincident with the jet superposition event. It is important to note that mixing ratios across the southern Mississippi River Valley and northern Gulf of Mexico were largely unchanged between the two days (not shown). As a result, the increase in poleward moisture flux was a direct consequence of an increase in wind speed. To investigate the impact of the superposed jet on the poleward moisture flux, we return to the cross section labeled C-C' in Fig. 7b, drawn perpendicular to the superposed jet axis and through the axis of maximum poleward moisture flux at 0000 UTC 2 May. The solution for the circulation within this cross section, shown in Fig. 12a, depicts a robust thermally indirect circulation, much stronger than the circulation associated solely with the subtropical jet at the previous time (Fig. 10a), and shifted towards the anticyclonic shear side of the jet. The superposed jet circulation is characterized by 1) a plume of ascent that extends from the surface through the jet core with local maxima found in both the middle and lower troposphere, and 2) much stronger moisture fluxes over the northern Gulf of Mexico, maximized around 15 cm s^{-1} near 925 hPa.

The cross section C-C' is oriented at an angle to the axis of maximum moisture flux at this time. Consequently, in order to facilitate a direct comparison between the poleward moisture fluxes associated with both the subtropical and the superposed jets, the component of the moisture flux associated with the superposed jet in the direction of the axis of maximum moisture flux at 0000 UTC 2 May was calculated and determined to be 11 cm s^{-1} at 925 hPa. This is an increase of about 6 cm s^{-1} (a 120% increase) from that associated solely with the subtropical jet at the earlier time. Figure 12b shows that this value is on par with, but slightly larger than, observed ageostrophic poleward moisture fluxes just south of New Orleans. This overestimate is at least partially a result of the fact that we neglect the effects of friction and flow curvature on the ageostrophic circulation in our solution of the Sawyer-Eliassen equation. Recalling that total ageostrophic moisture flux values increased by as much as 9 cm s^{-1} over the 24-h period (Fig. 9c), we conclude that the ageostrophic circulation associated with superposed jet accounts for the vast majority of the increased poleward moisture flux. As demonstrated by M12, this moisture flux was crucial in the production of precipitation further to the north during the flooding event. Thus, the analysis presented here illustrates the role the intensified Sawyer-Eliassen circulation associated with the superposed jet played in magnifying the severity of the event.

b. Partition of Sawyer-Eliassen Forcing Terms

The diagnostic power of the Sawyer-Eliassen equation (1) lies in the fact that the forcing can be broken down into the separate geostrophic forcing terms (shearing and stretching deformation) and a diabatic term. Consequently, the circulation associated with the superposed jet can be further dissected in order to gauge the significance of the respective forcing terms in shaping its sense and strength. The portion of the Sawyer-Eliassen circulation associated with the total geostrophic forcing (Q_g) is shown in Fig. 13a and depicts a circulation that, similar to the full circulation (Fig. 12a), is thermally indirect and shifted towards the anticyclonic shear side of the jet, positioning ascent directly beneath the jet core.

Intriguing differences, however, are found when comparing the distribution of the vertical motion and moisture flux to that shown in Fig. 12a. In contrast to the full circulation (Fig.

12a), which has a plume of ascent from the surface through the jet core, the Q_g circulation (Fig. 13a) has its strongest vertical motions primarily confined to the middle and upper troposphere. In addition, the low-level, horizontal branch of the Q_g circulation near the surface at the Gulf Coast is far weaker, with low-level moisture flux values only around 3 cm s^{-1}, much smaller than those forced by the full circulation.

The Q_g circulation, in Fig. 13a, can be partitioned into the individual circulations associated with the geostrophic shearing (Q_{SH}) and stretching (Q_{ST}) deformation terms, respectively. The Q_{SH} circulation is shown in Fig. 13b and depicts a thermally indirect circulation that is positioned primarily on the cyclonic shear side of the jet. This places the descending branch of the circulation directly beneath the jet core, opposite to the ascent observed in that region in the Q_g circulation. Examination of both the temperature gradient and geostrophic wind normal to the cross section suggests that areas between roughly 400-800 hPa were characterized by geostrophic cold air advection in cyclonic shear ($Q_{SH} < 0$), consistent with the thermally indirect characteristics of the circulation observed in Fig. 13b.

Figure 13c shows that Q_{ST} acts to drive a thermally direct circulation about the strong upper tropospheric front centered on the cyclonic shear side of the jet, but offset slightly poleward of the center of the Q_{SH} circulation (Fig. 13b). Consequently, Q_{ST} promotes ascent directly beneath the jet core, slightly poleward of, and thus counteracting, the subsidence associated with Q_{SH}. Investigation of the along-cross section geostrophic wind shows a region of geostrophic confluence centered squarely on the upper tropospheric front ($Q_{ST} > 0$), which would act to enhance the horizontal temperature gradient around 500 hPa and drive a thermally direct circulation.

Interestingly, this cross section is drawn through a geostrophic jet exit region at 500 hPa, as shown in Fig. 14. Typically, such regions are characterized by diffluent flow and associated horizontal frontolysis in the vicinity of any regions of baroclinicity, resulting in a thermally indirect circulation. Figure 14 shows that in this case, an embedded shortwave trough over the panhandles of Oklahoma and Texas actually produces a region of geostrophic confluence in the vicinity of the geostrophic jet exit region. This confluence is responsible for an area of horizontal geostrophic frontogenesis precisely in the location in which a thermally direct circulation is observed in Fig. 13c.

Comparison of the intensities and areal extents of the Q_{SH} and Q_{ST} circulations demonstrates that the Q_{SH} circulation is the dominant component. Consequently, the sum of the two circulations indicates that the Q_{ST} circulation acts to erode the updraft associated with the Q_{SH} circulation on the cyclonic shear side of the jet, while preserving the downdraft on the anticyclonic shear side. The net result remains a thermally indirect circulation, but one that is shifted towards the anticyclonic shear side of the jet with ascent directly beneath the jet core. This total Q_g circulation is displaced further equatorward than might be expected under a regime of geostrophic cold air advection in cyclonic shear within a geostrophic jet exit region (Fig. 5b) due to the effects of the geostrophic confluence associated with the shortwave trough.

The final contribution to the full Sawyer-Eliassen circulation comes from the diabatic forcing. Figure 15a shows that the circulation associated with the diabatic forcing is focused entirely below 400 hPa, where latent heating acts to produce a dipole centered slightly north of the Gulf Coast, with a thermally direct circulation further to the north and a stronger thermally indirect circulation to the south. Upward vertical motions associated with this diabatically-induced circulation are also focused in the lower troposphere and coincide well with the area of most intense latent heat release from the initial convective activity. Most notably, the poleward moisture flux associated with the thermally indirect diabatic circulation (Fig. 15a) is much stronger than that associated with the Q_g circulation (Fig. 13a), with values greater than 9 cm s^{-1} over the northern Gulf of Mexico. Consequently, the majority of the poleward moisture flux produced by the full ageostrophic circulation is driven by the diabatic component.

The preceding discussion indicates that the Q_g forcing largely determines the mid-tropospheric portion of the full Sawyer-Eliassen circulation (Fig. 12a). The diabatic portion, then, provides a means by which the full tropospheric-deep circulation communicates directly with the surface, as it was responsible for the majority of the increase in low-level poleward moisture flux into the southeast United States and also coupled surface-based vertical motions to those in the middle troposphere.

The analysis also suggests a crucial positive feedback mechanism that, on its own, may act to further strengthen and promote the longevity of the entire Sawyer-Eliassen circulation. Strong moisture flux and subsequent ascent promotes latent heat release through condensation. The latent heat release produces a lower tropospheric ageostrophic circulation that can further strengthen the poleward moisture flux into a region and, subsequently, increase the potential for additional latent heat release. The addition of middle and upper tropospheric ascent provided by the Q_g circulation to that induced by the diabatically-forced circulation promotes the vigorous and tropospheric-deep vertical motions necessary for the production of heavy precipitation and intense latent heat release. In addition, the strong latent heat release beneath the jet core can act to erode upper-level PV, helping to fortify the vertical PV wall associated with the superposed jet structure thereby acting to maintain, or even strengthen, the strong wind speeds that are associated with it.

Support for the veracity of the superposed jet's diagnostic Sawyer-Eliassen circulation is also evident in the cross section of vertical motion from the GFS analysis, shown in Fig. 15b. Similar to the tropospheric-deep plume of ascent observed with the full superposed jet circulation in Fig. 12a, the GFS shows a continuous plume of ascent that runs roughly parallel to the leading edge of the upper tropospheric front and through the jet core. In addition, the distribution of vertical motion depicts two local maxima, one near the Gulf Coast in the vicinity of the maximum latent heat release (Fig. 15a), and another in the middle-to-upper troposphere that is nearly collocated with the maximum in ascent associated with the Q_g portion of the superposed jet circulation (Fig. 13a).

A similar positive feedback mechanism, envisioned from a PV perspective, was proposed by Lackmann (2002) in his study of a warm conveyor belt during a February 1997 cyclogenesis event and serves as an analog to the mechanism discussed above. In that case, it was found that the circulation associated with a linear, diabatically-generated positive PV anomaly along a low-level frontal boundary made a non-negligible contribution to the strength of the southerly low-level jet. The strengthened low-level jet then accomplished additional poleward moisture transport into the region, further conditioning the atmosphere for additional latent heat release. Indeed, Lackmann (2013) found similar conditions at work during the Nashville flood, where the low-level jet was characterized by a linear positive PV anomaly to its west, along the stationary cold frontal boundary. While the study indicated that topographic effects along the Mexican Plateau were the primary mechanism behind the initial generation of low-level cyclonic PV present along the frontal boundary during the event, diabatic effects acted to enhance the magnitude of these anomalies as they drifted eastward into the southern United States.

5. Discussion and Conclusions

The analysis presented here demonstrates that the lower tropospheric horizontal branch of the Sawyer-Eliassen circulation associated with a superposed jet helped to enhance the poleward moisture flux prior to the second day of the 2010 Nashville flood event. This explanation accounts for the analyses by M12 and Durkee et al. (2012) and their particular observations of increased poleward moisture transport during the second day of the event. Mixing ratios on these two days were largely unchanging across the southern Mississippi River Valley. Given this fact, an increased wind speed underlies the increased poleward moisture flux that was observed on the second day. The analysis presented here shows that this increased wind speed is primarily attributable to the ageostrophic circulation associated with the superposed jet and illuminates one mechanism by which such superposed jet structures may have an influence on the evolution of a high-impact weather event. Such a dynamical influence is undoubtedly magnified by the fact that the superposed circulation, by virtue of its association with the subtropical jet, is able to draw upon the moist and weakly stratified air mass characteristic of the lower troposphere equatorward of the subtropical jet.

Additionally, partition of the forcings driving the superposed jet circulation provides insights into its internal dynamics. In the case presented here, the Q_{SH} term was more dominant than the Q_{ST} term. As a result, the entire Q_g circulation took on the thermally indirect characteristics of the Q_{SH} circulation. The thermally direct circulation associated with the Q_{ST} forcing, however, acted to significantly counteract the Q_{SH} circulation on the cyclonic shear side of the jet, shifting the locus of the entire Q_g circulation towards the anticyclonic shear side of the jet. Such an orientation can dynamically assist convection, as upward vertical motions on the anticyclonic shear side of the jet are exhausted in an area with much lower inertial stability. In comparison to the cases examined by Shapiro (1981) and Shapiro (1982), this observed circulation is atypical for an environment of geostrophic cold air advection in a geostrophic jet exit region. It is important to note, however, that throughout much of the evolution of a superposed jet structure, the environment is characterized by more than one jet core. Therefore, idealized models of transverse circulations in environments characterized by single jet cores may not be expected to represent the circulations characterizing the more complex superposed jet environment.

Given that superposed jets are often characterized by anomalously strong wind speeds in the jet core, it is likely that the horizontal shear is also anomalously large in the vicinity of these features. Consequently, it is conceivable that the Q_{SH} term may consistently dominate the Q_g forcing for ageostrophic circulations associated with superposed jets, particularly away from geostrophic jet entrance and exit regions. A more comprehensive examination of other superposed jet streaks may illuminate the nature of the interaction between the two geostrophic forcing terms in the vicinity of these structures and how their circulations compare with established conceptual models.

Moreover, this case illustrates that latent heat release can have a considerable impact on shaping and enhancing the entire ageostrophic circulation. If they couple favorably, the Q_g

and diabatic circulations can drive a notable positive feedback mechanism, similar to that proposed by Lackmann (2002), which can act to both strengthen upward vertical motions and intensify the ageostrophic winds in the low-level horizontal branch of the circulation. Studies of jet circulations in other heavy precipitation events may help to further characterize this feedback mechanism.

Both Q_g circulations and latent heat release also have the ability to reshape the tropopause and, subsequently, affect the structure of the jet. The development of superposition events, in particular, is usually characterized by 1) the melding of two separate tropopause folds associated with the separate jets into a single, steeper one and 2) an attendant acceleration of the jet. We hypothesize that these transformations result from an interaction between latent heat release and internal jet-front dynamics. Figure 16 shows an idealized schematic in which both the polar and the subtropical jets are characterized by separate positive tropopause PV anomalies and cyclonic circulations that, while maximized at the level of the respective anomalies, extend vertically through their respective columns. When these anomalies come in close proximity to one another, their circulations can interact with a potential for destructive interference in the space between the separate jet cores, diminishing wind speeds in that location. Constructive interference in the column previously located between the two jets occurs when the two anomalies become vertically superposed and the tropopause steepens, producing the rapid acceleration of jet wind speeds and intensification of the secondary circulation that may be characteristic of a superposition event.

Latent heating from lower tropospheric frontal convection, which erodes upper-level PV, can promote steepening of the tropopause on the equatorward side of the subtropical jet. At the same time, stratospheric geostrophic warm air advection in cyclonic shear, as was present in the Nashville case both before and at the time of jet superposition (Fig. 13b), promotes ascent through the jet core via the Q_{SH} term, with subsidence poleward of the subtropical jet's exit region in the lower stratosphere (Lang and Martin 2012). This subsidence can act to flatten the PV trough in the space between the two jets, resulting in a single, more intensely sloped tropopause, the superposition of the two PV anomalies (jets), and subsequent, rapid accelerations in jet wind speeds and the attendant ageostrophic circulations. The initial latitudinal separation of the two jet cores is hypothesized to be critical in this process. If they are so far apart as to place the lower tropospheric convection between the two jets, the convection may actually inhibit superposition by strengthening and reinforcing the PV trough between the two jets. Work is ongoing to investigate the nature of the processes that contribute to jet superposition and to what degree these processes are dependent upon, and sensitive to, characteristic distributions of latent heat release.

Consideration of this problem via the piecewise PV inversion scheme of Davis and Emanuel (1991) is also currently underway. We are devising analysis schemes by which the respective PV anomalies associated with both the polar and subtropical jets can be isolated and individually inverted in order to determine the circulations associated with each anomaly. Interactions between these separate circulations, and their individual ability to reshape the tropopause into the two-step structure characteristic of jet superpositions, will provide considerable insight into the process of superposition. The role of latent heat and surface-based PV anomalies can, in a similar manner, be interrogated from the PV perspective, assisting in the development of a comprehensive picture of the dynamics driving jet superpositions. The results from this particular case study demonstrate that such features can, indeed, play a central role in the evolution of high-impact weather events. Consequently, greater understanding of the processes that conspire to form superposed jet structures, via consideration of internal jet-front dynamics from either the basic-state variables or PV perspectives, can better inform forecasters regarding both the operation of such features as well as anticipation of their impacts.

Acknowledgments.

This work was supported by the National Science Foundation through grant NSF-0950349. The authors are grateful for the thoughtful and constructive reviews of three anonymous reviewers, which have resulted in a much improved manuscript.

REFERENCES

Barnes, S. L. and B. R. Colman, 1993: Quasigeostrophic diagnosis of cyclogenesis associated with a cutoff extratropical cyclone - the Christmas 1987 storm. *Mon. Wea. Rev.*, **121**, 1613–1634.

Bolton, D., 1980: The computation of equivalent potential temperature. *Mon. Wea. Rev.*, **108**, 1046–1053.

Bryan, G. H., 2008: On the computation of pseudoadiabatic entropy and equivalent potential temperature. *Mon. Wea. Rev.*, **136**, 5239–5245.

Davis, C. A. and K. A. Emanuel, 1991: Potential vorticity diagnostics of cyclogenesis. *Mon. Wea. Rev.*, **119**, 1929–1953.

Defant, F. and H. Taba, 1957: The threefold structure of the atmosphere and the characteristics of the tropopause. *Tellus*, **9**, 259–275.

desJardins, M. L., K. F. Brill, and S. S. Schotz, 1991: Use of GEMPAK on UNIX workstations. *7th Int. Conf. on Interactive Information and Processing Systems for Meteorology, Oceanography, and Hydrology*, New Orleans, LA, Amer. Meteor. Soc., 449–453.

Durkee, J. D., L. Campbell, K. Berry, D. Jordan, G. Goodrich, R. Mahmood, and S. Foster, 2012: A synoptic perspective of the record 1-2 May 2010 mid-South heavy precipitation event. *Bull. Amer. Meteor. Soc.*, **93**, 611–620.

Eliassen, A., 1962: On the vertical circulation in frontal zones. *Geophys. Publ.*, **24**, 147–160.

Emanuel, K. A., M. Fantini, and A. J. Thorpe, 1987: Baroclinic instability in an environment of small stability to slantwise moist convection. Part I: Two-dimensional models. *J. Atmos. Sci.*, **44**, 1559–1573.

Guan, B., N. P. Molotch, D. E. Waliser, E. J. Fetzer, and P. J. Neiman, 2010: Extreme snowfall events linked to atmospheric rivers and surface air temperature via satellite measurements. *Geophys. Res. Lett.*, **37**, L20401, doi:10.1029/2010GL044696.

Hobbs, P. V., J. D. Locatelli, and J. E. Martin, 1990: Cold fronts aloft and forecasting of precipitation and severe weather east of the Rocky Mountains. *Wea. Forecasting*, **5**, 613–626.

Keyser, D. and M. J. Pecnick, 1985: A two-dimensional primative equation model of frontogenesis forced by confluence and horizontal shear. *J. Atmos. Sci.*, **42**, 1259–1282.

Keyser, D. and M. A. Shapiro, 1986: A review of the structure and dynamics of upper-level frontal zones. *Mon. Wea. Rev.*, **114**, 452–499.

Koteswaram, P., 1953: An analysis of the high tropospheric wind circulation over India in winter. *Indian J. Meteor. Geophys.*, **4**, 13–21.

Koteswaram, P. and S. Parthasarathy, 1954: The mean jet stream over India in the pre-monsoon and post-monsoon seasons and vertical motions associated with subtropical jet streams. *Indian J. Meteor. Geophys.*, **5**, 138–156.

Krishnamurti, T. N., 1961: The subtropical jet stream of winter. *J. Meteor.*, **18**, 172–191.

Lackmann, G. M., 2002: Potential vorticity redistribution, the low-level jet, and moisture transport in extratropical cyclones. *Mon. Wea. Rev.*, **130**, 59–74.

Lackmann, G. M., 2013: The south-central U.S. flood of May 2010: Present and future. *J. Climate*, **26**, 4688–4709.

Lackmann, G. M., D. Keyser, and L. F. Bosart, 1997: A characteristic life cycle of upper-tropospheric cyclogenetic precursors during Experiment on Rapidly Intensifying Cyclones of the Atlantic (ERICA). *Mon. Wea. Rev.*, **125**, 2729–2758.

Lang, A. A. and J. E. Martin, 2012: The structure and evolution of lower stratospheric frontal zones. Part I: Examples in northwesterly and southwesterly flow. *Quart. J. Roy. Meteor. Soc.*, **138**, 1350–1365.

Loewe, F. and V. Radok, 1950: A meridional aerological cross section in the Southwest Pacific. *J. Meteor.*, **7**, 58–65, (Revised 305-306).

Lynch, S. and R. Schumacher, 2013: Ensemble-based analysis of the May 2010 extreme rainfall in Tennessee and Kentucky. *Mon. Wea. Rev.,*, doi:10.1175/MWR-D-13-00020.1, in press.

Martin, J. E., 2014: Quasi-geostrophic diagnosis of the influence of vorticity advection on the development of upper level jet-front systems. *Quart. J. Roy. Meteor. Soc.*, **140**, submitted.

Martin, J. E., J. D. Locatelli, and P. V. Hobbs, 1993: Organization and structure of clouds and precipitation on the mid-Atlantic coast of the United States. Part VI: The synoptic evolution of a deep tropospheric frontal circulation and attendant cyclogenesis. *Mon. Wea. Rev.*, **121**, 1299–1316.

Mohri, K., 1953: On the fields of wind and temperature over Japan and adjacent waters during winter of 1950-1951. *Tellus*, **5**, 340–358.

Moore, B. J., P. J. Neiman, F. M. Ralph, and F. E. Barthold, 2012: Physical processes associated with heavy flooding rainfall in Nashville, Tennessee, and vicinity during 1-2 May 2010: The role of an atmospheric river and mesoscale convective systems. *Mon. Wea. Rev.*, **140**, 358–378.

Namias, J. and P. F. Clapp, 1949: Confluence theory of the high tropospheric jet stream. *J. Meteor.*, **6**, 330–336.

National Weather Service, 2011: Record floods of Greater Nashville: Including flooding in middle Tennessee and western Kentucky, May 1-4, 2010. NWS Service Assessment, 93 pp. [Available online at http://www.weather.gov/os/assessments/pdfs/Tenn_Flooding.pdf].

Newell, R. E., N. E. Newell, Y. Zhu, and C. Scott, 1992: Tropospheric rivers? - A pilot study. *Geophys. Res. Lett.*, **19**, 2401–2404.

Newton, C. W., 1954: Frontogenesis and frontolysis as a three-dimensional process. *J. Meteor.*, **11**, 449–461.

Omoto, Y., 1965: On pre-frontal precipitation zones in the United States. *J. Meteor. Soc. Japan*, **43**, 310–330.

Palmén, E. and C. W. Newton, 1948: A study of the mean wind and temperature distribution in the vicinity of the polar front in winter. *J. Meteor.*, **5**, 220–226.

Palmén, E. and C. W. Newton, 1969: *Atmospheric Circulation Systems: Their Structure and Physical Interpretation*. Academic Press, 603 pp.

Ralph, F. M., P. J. Neiman, G. A. Wick, S. I. Gutman, M. D. Dettinger, D. R. Cayan, and A. B. White, 2006: Flooding on California's Russian River: Role of atmospheric rivers. *Geophys. Res. Lett.*, **33**, L13801, doi:10.1029/2006GL026689.

Reed, R. J., 1955: A study of a characteristic type of upper-level frontogenesis. *J. Meteor.*, **12**, 226–237.

Reed, R. J. and F. Sanders, 1953: An investigation of the development of a mid-tropospheric frontal zone and its associated vorticity field. *J. Meteor.*, **10**, 338–349.

Riehl, H., 1962: Jet streams of the atmosphere. Technical Report No. 32, Department of Atmospheric Science, Colorado State University, Fort Collins, CO, 117 pp.

Sawyer, J. S., 1956: The vertical circulation at meteorological fronts and its relation to frontogenesis. *Proceedings of the Royal Society of London*, **A234**, 346–362.

Shapiro, M. A., 1981: Frontogenesis and geostrophically forced secondary circulations in the vicinity of jet stream-frontal zone systems. *J. Atmos. Sci.*, **38**, 954–973.

Shapiro, M. A., 1982: *Mesoscale Weather Systems of the Central United States*. CIRES Univ. of Colorado/NOAA, Boulder, CO, USA, 78 pp.

Shapiro, M. A. and D. Keyser, 1990: Fronts, jet streams, and the tropopause. *Extratropical Cyclones: The Erik Palmén Memorial Volume*, C. Newton and E. O. Holopainen, Eds., Amer. Meteor. Soc., 167–191.

Stohl, A., C. Forster, and H. Sodemann, 2008: Remote sources of water vapor forming precipitation on the Norwegian west coast at 60°N: A tale of hurricanes and an atmospheric river. *J. Geophys. Res.*, **113**, D05102, doi:10.1029/2007JD009006.

Sutcliffe, R. C., 1947: A contribution to the problem of development. *Quart. J. Roy. Meteor. Soc.*, **73**, 370–383.

Sutcliffe, R. C. and J. K. Bannon, 1954: Seasonal changes in the upper-air conditions in the Mediterranean Middle East area. *Sci. Proc. International. Assoc. Meteor. (UGGI)*, Rome 1954.

Todsen, M., 1964: A computation of the vertical circulation in a frontal zone from the quasi-geostrophic equations. Technical Note No. 4, Air Force Cambridge Laboratories. OAR Contr. No. AF 61(052)-525.

Uccellini, L. W. and D. R. Johnson, 1979: The coupling of upper and lower tropospheric jet streaks and implications for the development of severe convective storms. *Mon. Wea. Rev.*, **107**, 682–703.

Uccellini, L. W., D. Keyser, K. F. Brill, and C. H. Wash, 1985: The President's Day cyclone of 18-19 February 1979: Influence of upstream trough amplification and associated tropopause folding on rapid cyclogenesis. *Mon. Wea. Rev.*, **113**, 962–988.

Uccellini, L. W. and P. J. Kocin, 1987: The interaction of jet streak circulations during heavy snow events along the east coast of the United States. *Wea. Forecasting*, **2**, 289–308.

Uccellini, L. W., P. J. Kocin, R. A. Petersen, C. H. Wash, and K. F. Brill, 1984: The President's Day cyclone of 18-19 February 1979: Synoptic overview and analysis of the subtropical jet streak influencing the pre-cyclogenetic period. *Mon. Wea. Rev.*, **112**, 31–55.

Whitaker, J. S., L. W. Uccellini, and K. F. Brill, 1988: A model based diagnostic study of the rapid development phase of the President's Day Cyclone. *Mon. Wea. Rev.*, **116**, 2337–2365.

Yeh, T. C., 1950: The circulation of the high troposphere over China in the winter of 1945-46. *Tellus*, **2**, 173–183.

Zhu, Y. and R. E. Newell, 1998: A proposed algorithm for moisture fluxes from atmospheric rivers. *Mon. Wea. Rev.*, **126**, 725–735.

List of Figures

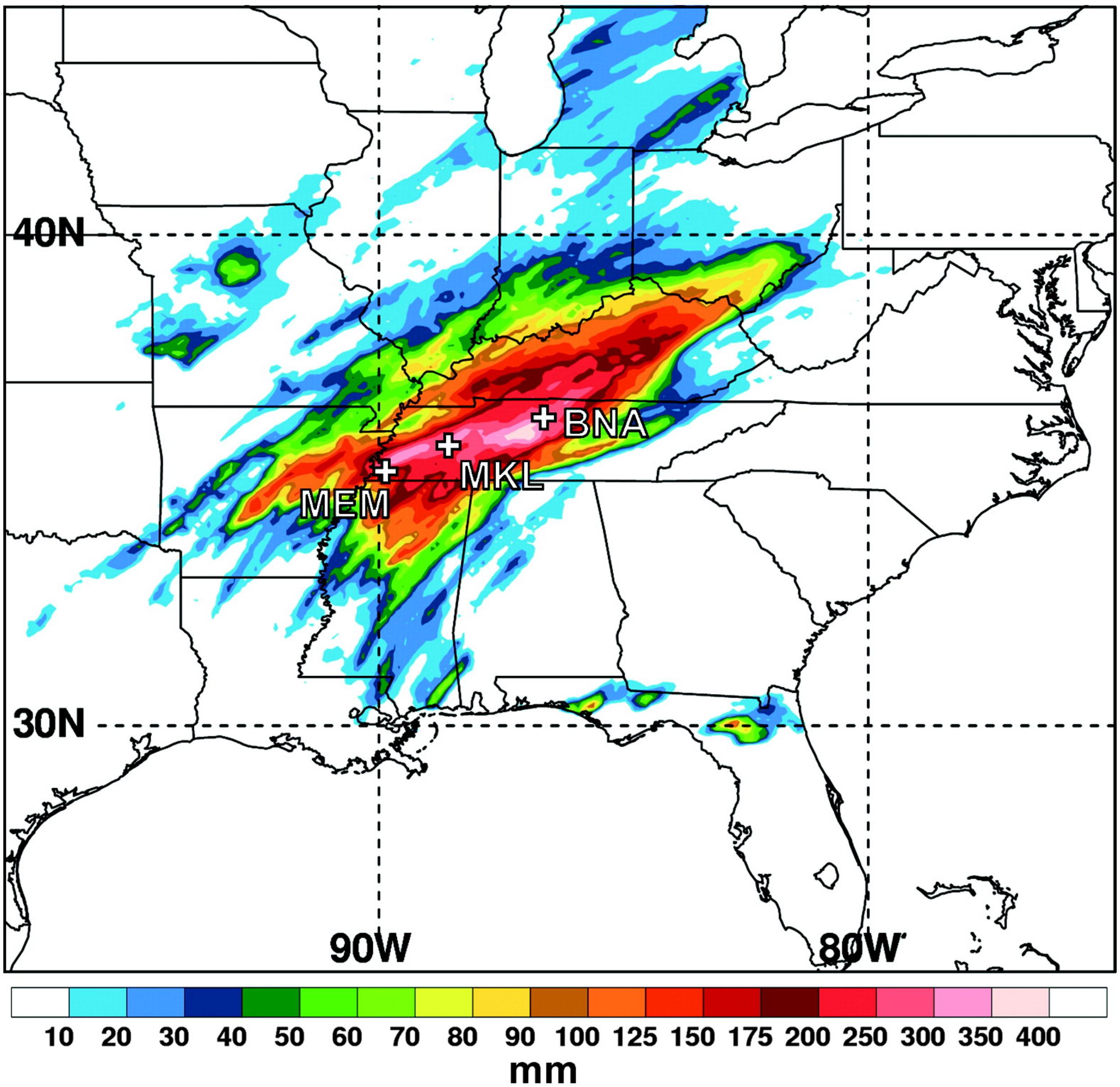

FIG. 1. 48-h precipitation estimates (shaded in mm following the color bar) for 0000 UTC 1 May - 0000 UTC 3 May 2010 from the National Precipitation Verification Unit quantitative precipitation estimates product. The location of Nashville (BNA), as discussed in the text, is identified. [From Moore et al. (2012; their Fig. 2)]

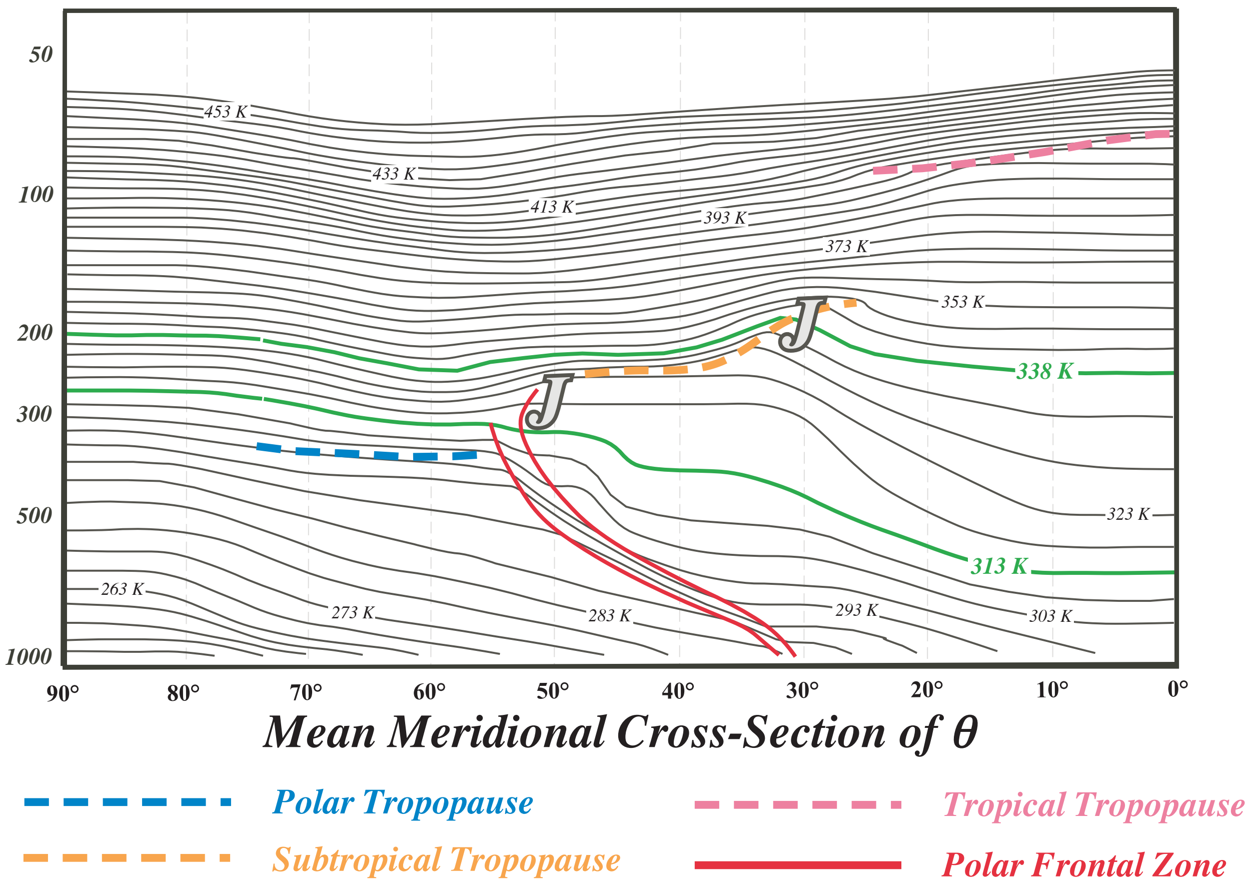

FIG. 2. Mean meridional cross section of potential temperature for 1 January 1956 with the polar, subtropical, and tropical tropopauses and polar frontal zone labeled as indicated in the legend. (Modified from Defant and Taba 1957; Fig. 13)

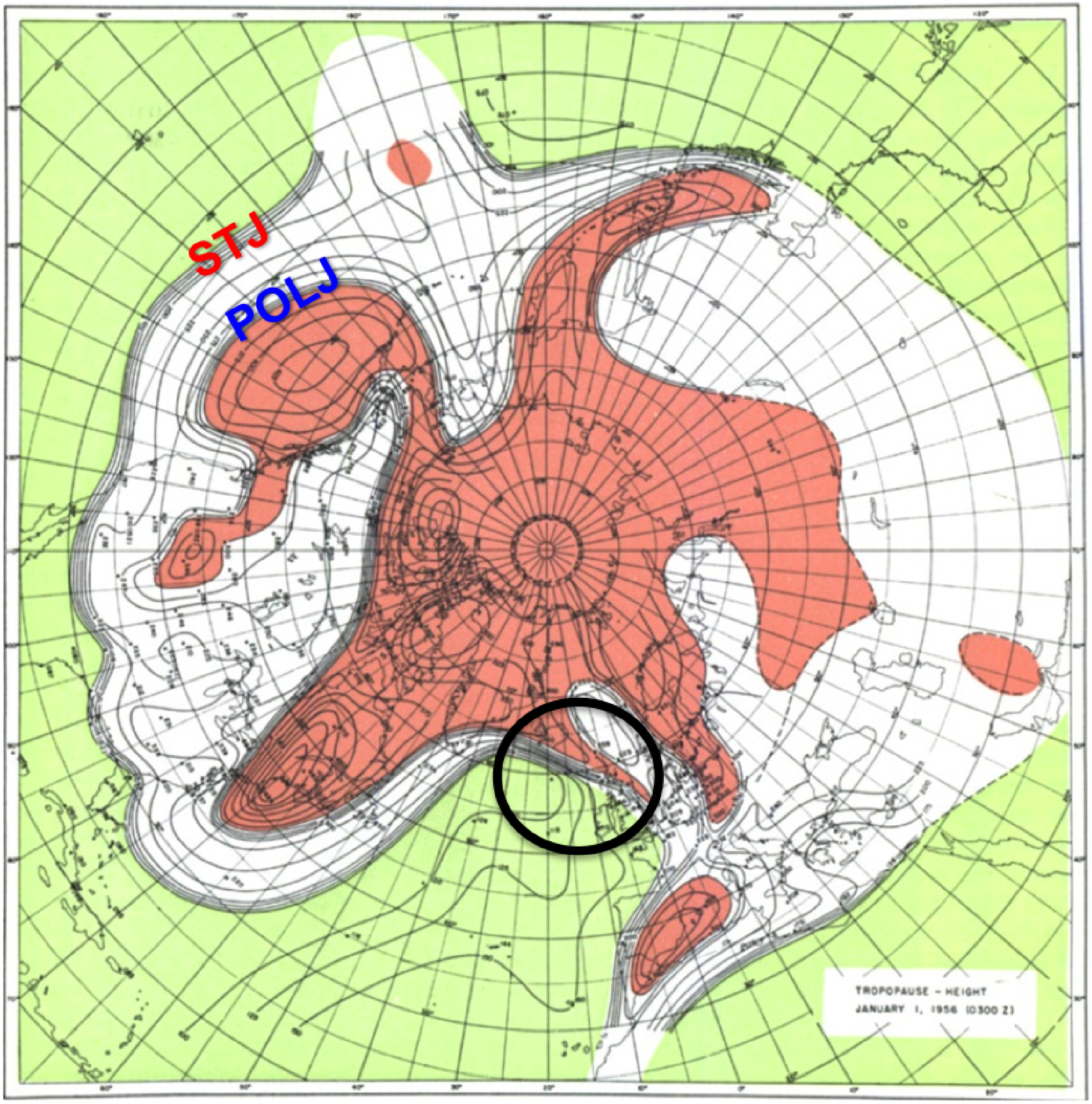

FIG. 3. Northern hemispheric map of tropopause height (hPa) at 0300 UTC 1 January 1956. Breaklines are denoted as areas with a sharp gradient in tropopause height. Breaklines that correspond to the subtropical (STJ) and polar jet (POLJ) are labeled accordingly. Area denoted with a circle is a region characterized by a superposition of the polar and subtropical jet. Green shading corresponds to the tropical tropopause, white shading the subtropical tropopause, and red the polar tropopause. (Modified from Defant and Taba 1957; Fig. 2)

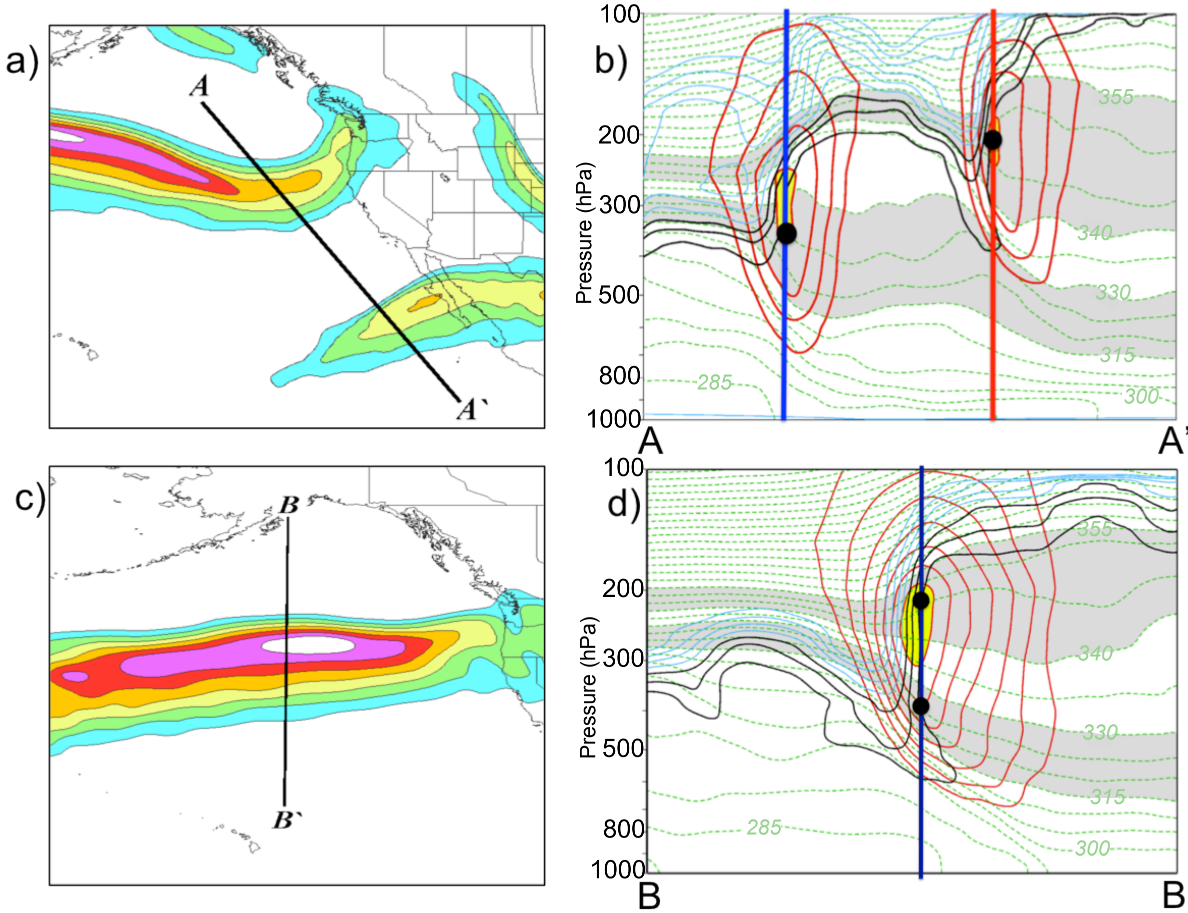

FIG. 4. (a) 300 hPa isotachs (shaded every 10 m s^{-1} starting at 30 m s^{-1}) at 0000 UTC 27 April 2010 depicting separate polar and subtropical jets. (b) Cross section from A-A', in Fig. 4a, through separate polar and subtropical jet cores with contours of the 1,2,3 PVU (1 PVU = K m^2 kg^{-1} s^{-1}) surfaces (black), 4,5,6,7,8,9, PVU surfaces (light blue), potential temperature every 5K (dashed green), and isotachs every 10 m s^{-1} beginning at 30 m s^{-1} (red). The jet core is shaded yellow and the 315-330K and 340-355K isentropic layers, used to identify the location of the jets, are shaded gray. The blue (red) column corresponds to a grid column with the black dot confirming a positive ID of a polar (subtropical) jet. (c) Same as (a) depicting a superposed jet at 0000 UTC 24 October 2010. (d) Same as (b) but for the cross section from B-B', in Fig. 4c, with two positive IDs (black dots) within a single grid column indicating a jet superposition.

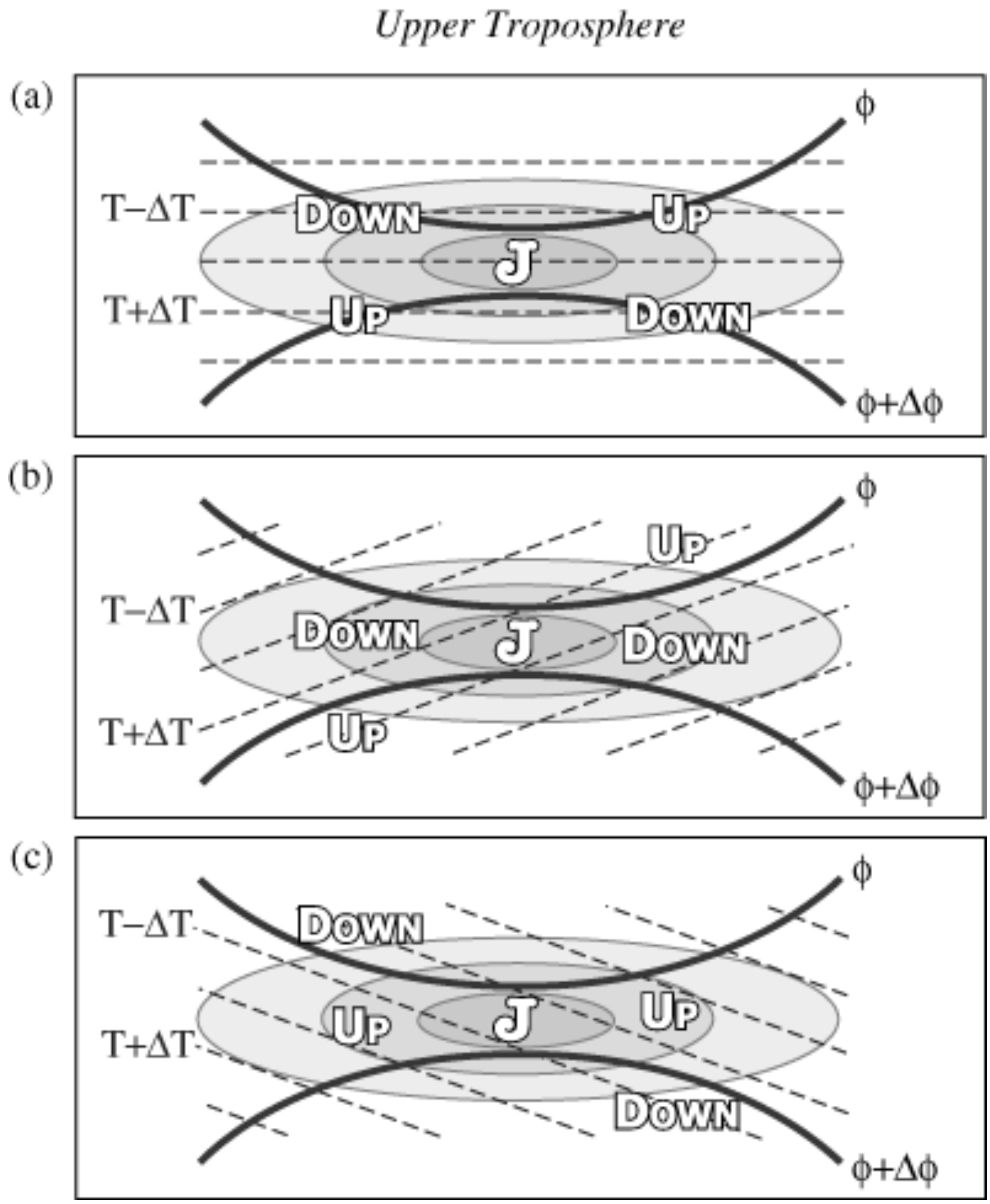

FIG. 5. Idealized configurations of jet circulations associated with a straight jet streak on an isobaric surface in the upper troposphere. Geopotential height (thick solid lines), potential temperature (dashed lines), geostrophic isotachs (fill pattern; with the jet speed maximum represented by the "J"), and Sawyer-Eliassen vertical motions indicated by "up" and "down" for a regime of (a) no geostrophic temperature advection (b) upper tropospheric geostrophic cold air advection and (c) upper tropospheric geostrophic warm air advection along the jet axis. (From Lang and Martin 2012; Fig. 3)

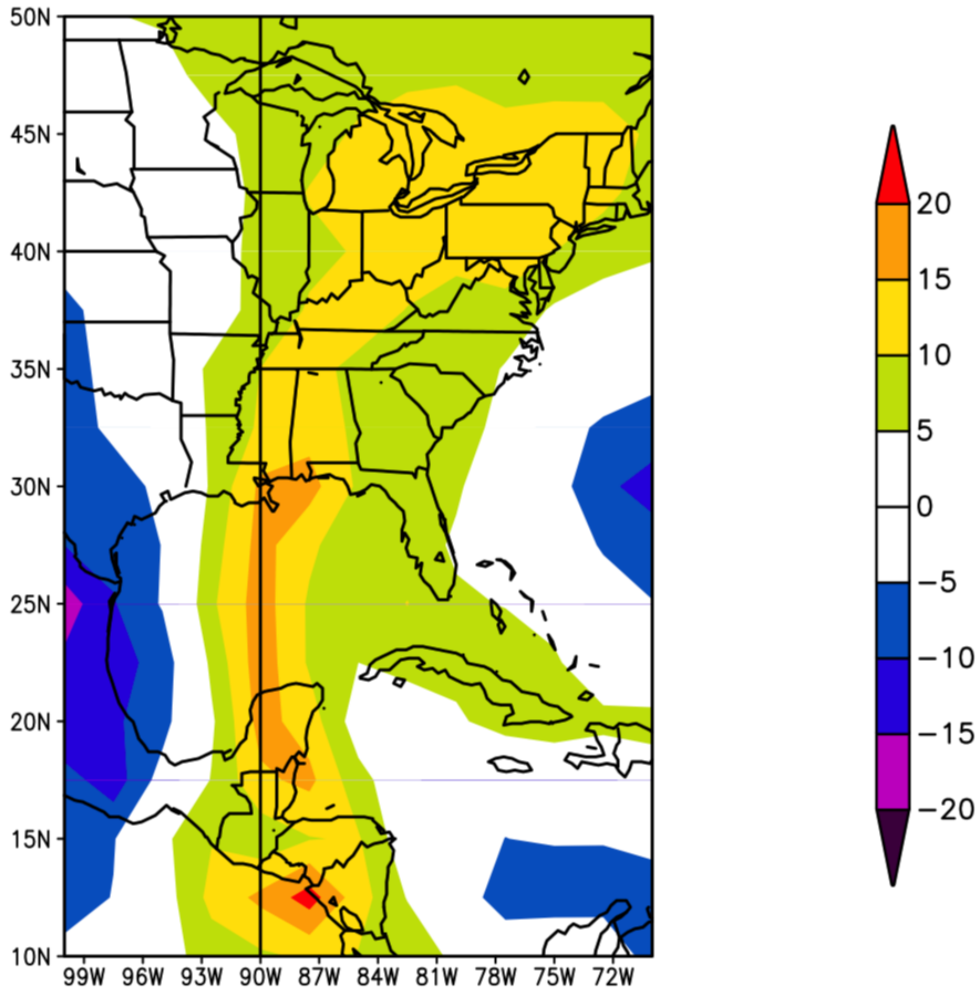

Fig. 6. 4-day precipitable water anomalies in mm (fill pattern) during the period of 30 April 2010 - 3 May 2010 across the eastern United States. (Earth Systems Research Lab)

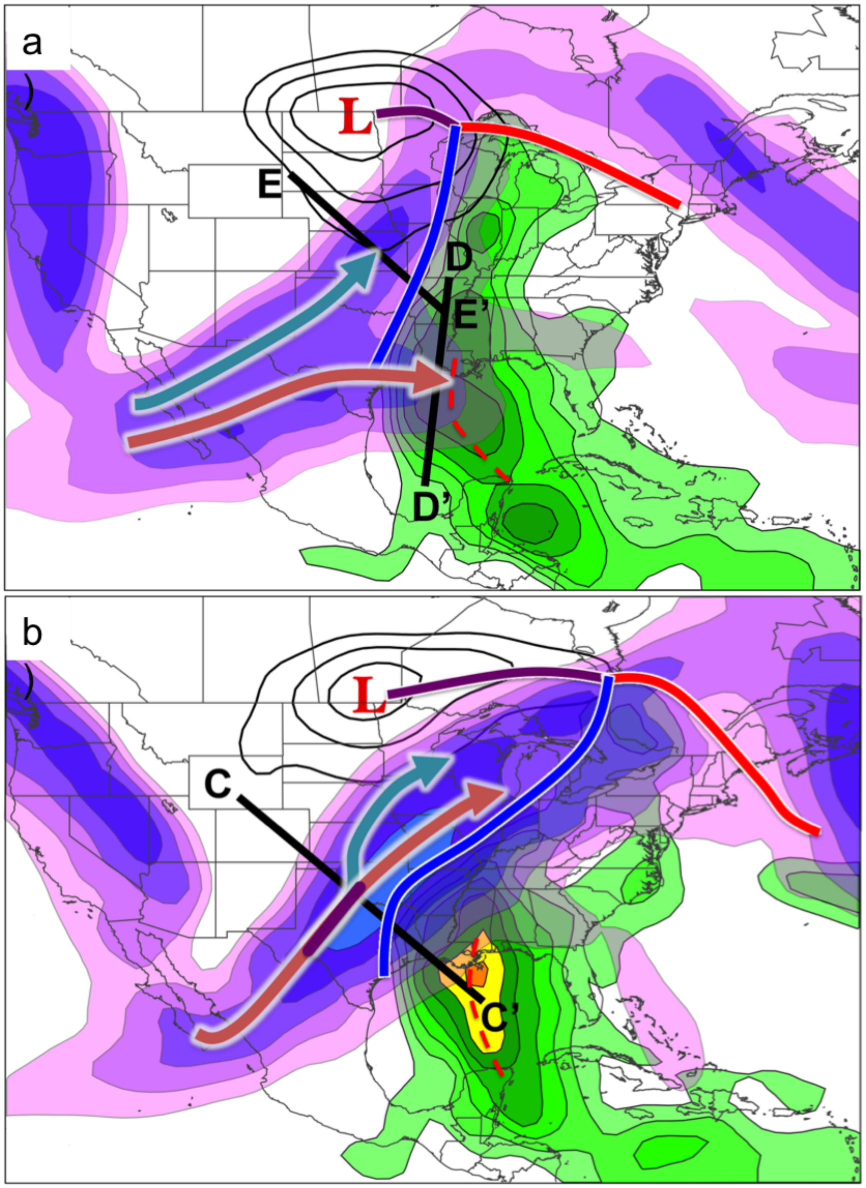

Fig. 7. Synoptic overview with sea-level pressure every 4 hPa beginning at 996 hPa (thin black lines), surface low pressure center (red "L"), surface frontal boundaries with the cold front denoted by the blue line, the warm front in red, and occluded front in purple, magnitude of the 925 hPa poleward moisture flux every 5 cm s^{-1} beginning at 10 cm s^{-1} (green fill pattern), 250 hPa isotachs every 10 m s^{-1} beginning at 30 m s^{-1} (purple fill pattern), the location of the polar (blue arrow), subtropical (red arrow), and superposed (purple line) jet, as identified using the algorithm defined in the text, and the axis of maximum 925 hPa poleward moisture flux (red dashed line) at (a) 0000 UTC 1 May 2010 and (b) 0000 UTC 2 May 2010.

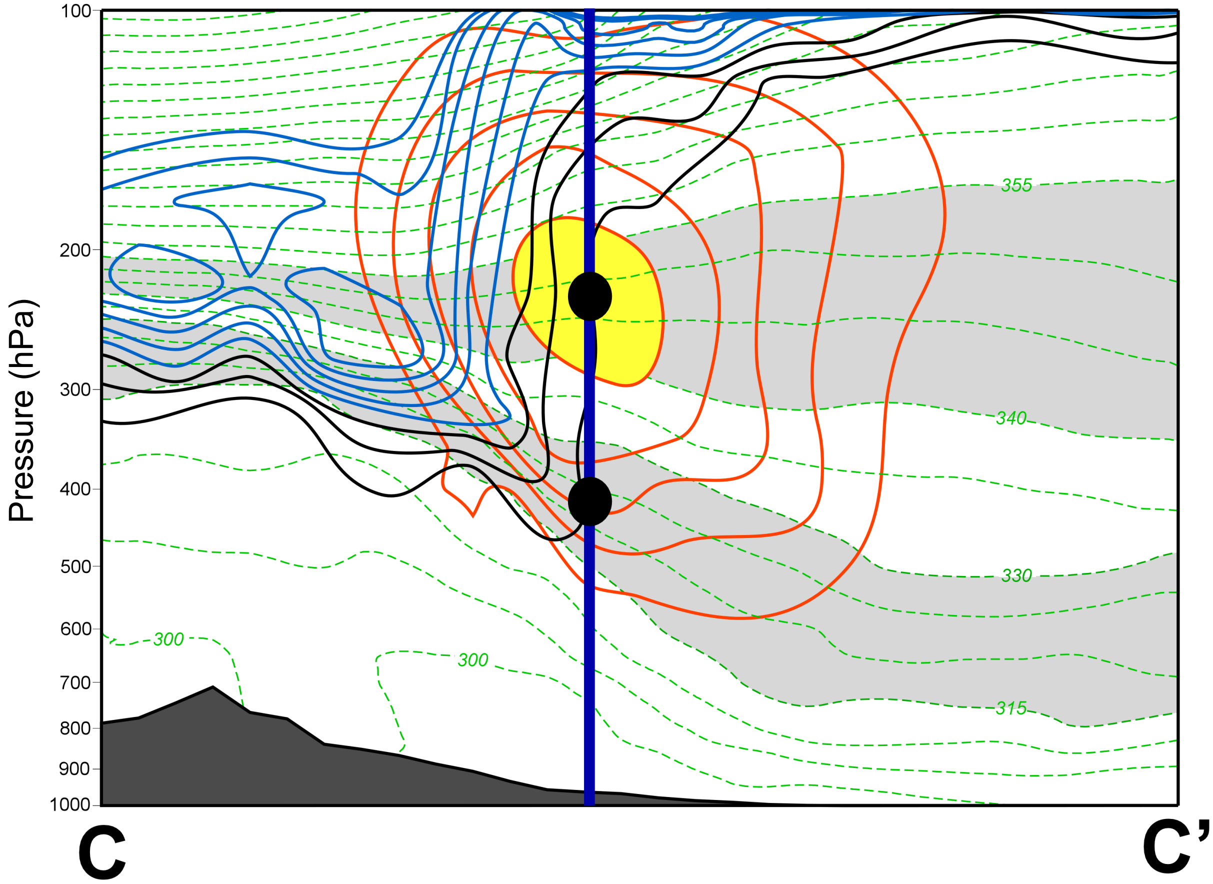

Fig. 8. Vertical cross section of potential temperature, potential vorticity, and isotachs at 0000 UTC 2 May 2010 along the line C-C’ in Fig. 7b. Variables labeled, contoured, and shaded as in Fig. 4d. Black dots represent separate polar and subtropical jet identifications in the same grid column, which is identified by the bold vertical line.

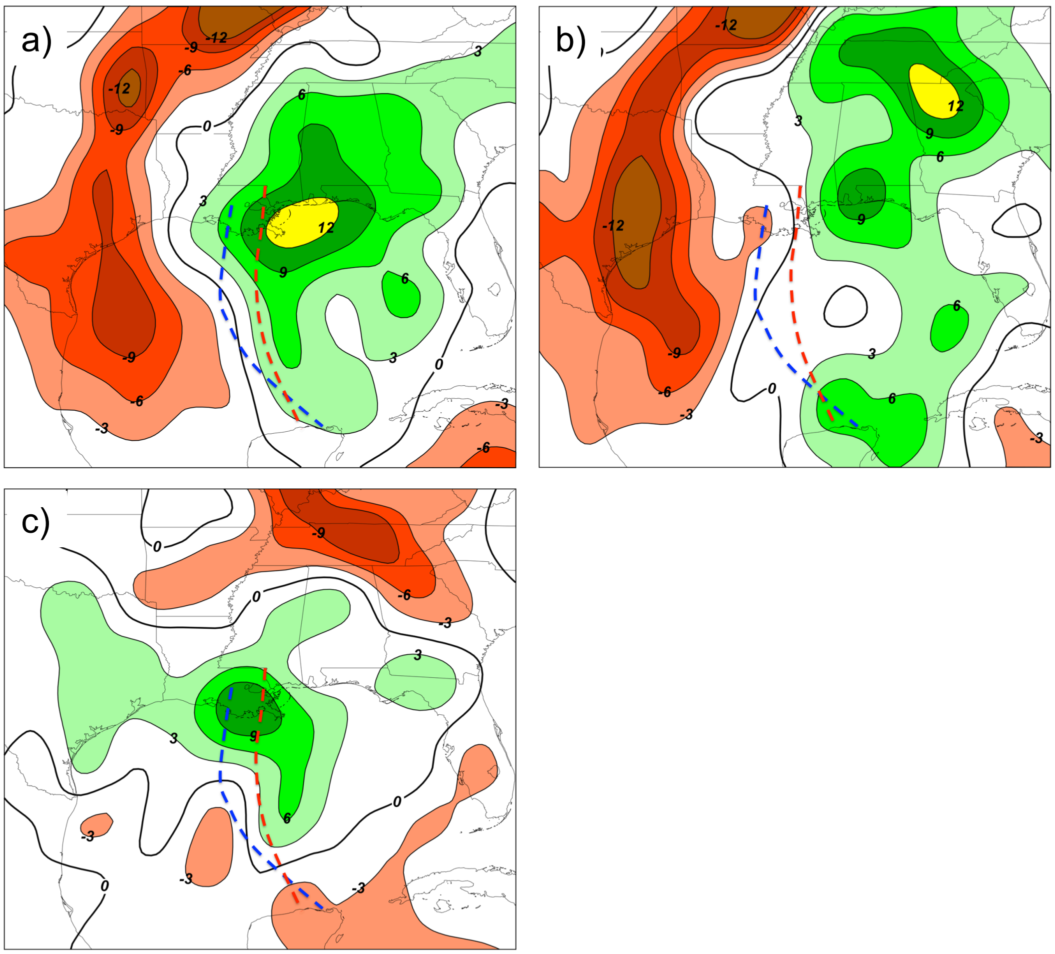

FIG. 9. Change in the magnitude of the 925 hPa (a) total, (b) geostrophic, and (c) ageostrophic poleward moisture flux over the Southeast U.S. during the 24-h period from 0000 UTC 1 May to 0000 UTC 2 May. Changes in the moisture flux greater than (less than) 3 (-3) cm s^{-1} are shaded in the green (red/brown) fill pattern every 3 cm s^{-1} with 0 cm s^{-1} contoured in black. Blue (red) dashed line represents the axis of maximum poleward moisture flux at 0000 UTC 1 May (2 May), as indicated in Fig. 7

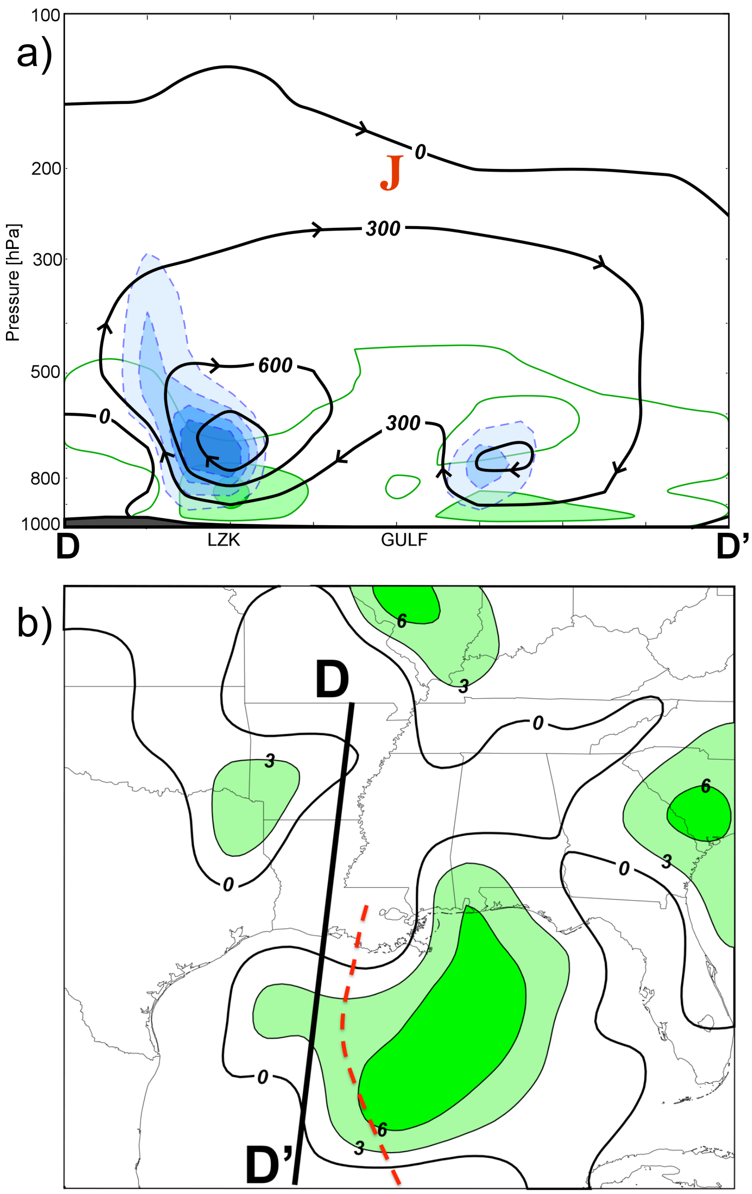

FIG. 10. (a) Cross section along the line D-D', in Fig. 7a, at 0000 UTC 1 May of Sawyer-Eliassen streamfunction every 300 m hPa s^{-1} (black lines), moisture flux associated with the Sawyer-Eliassen circulation every 3 cm s^{-1} beginning at 0 cm s^{-1} (0 cm s^{-1} is contoured in green with the green fill pattern used for values greater than 3 cm s^{-1}), and negative omega associated with the Sawyer-Eliassen circulation every 1 dPa s^{-1} beginning at 1 dPa s^{-1} (blue fill pattern, dashed contours). The sense of the circulation is depicted by the arrowheads plotted on the streamfunction contours, the location of the subtropical jet core is indicated by the "J", and GULF represents the Gulf Coast. (b) 925 hPa ageostrophic poleward moisture flux every 3 cm s^{-1} beginning at 0 cm s^{-1} (0 cm s^{-1} is contoured in black with the green fill pattern used for values greater than 3 cm s^{-1}) and the axis of maximum poleward moisture flux (red dashed line previously indicated on Fig. 7a) at 0000 UTC 1 May.

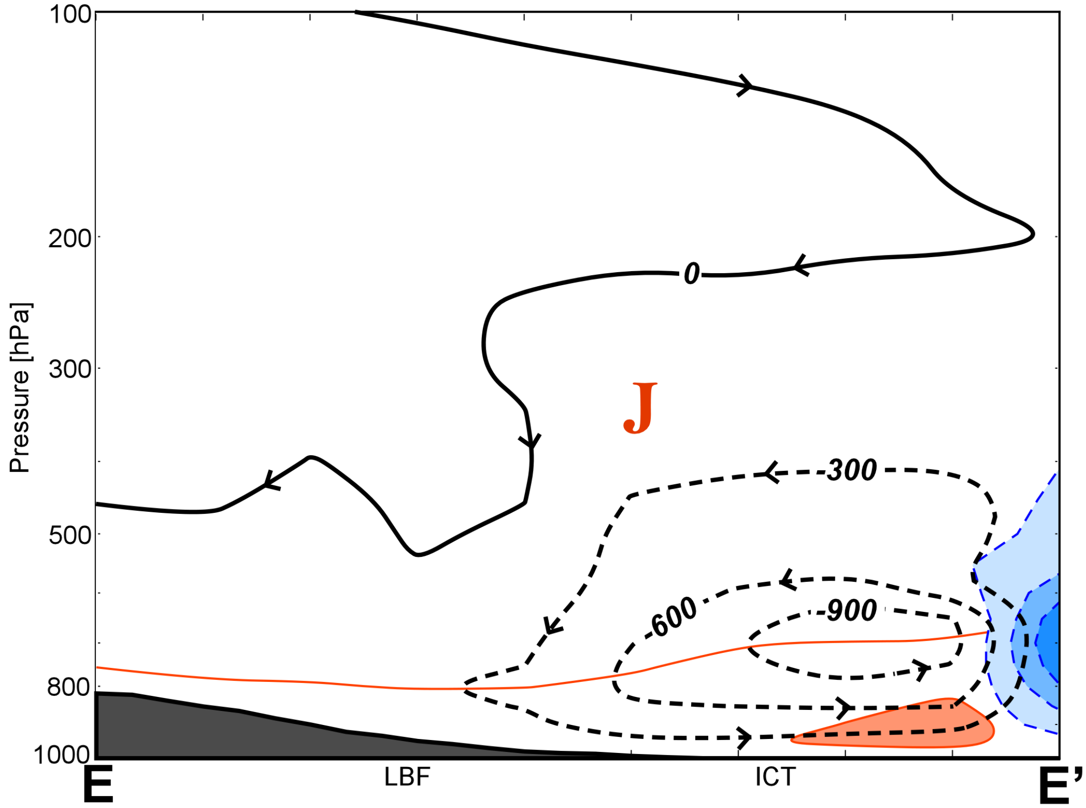

FIG. 11. Cross section along the line E-E', in Fig. 7a, at 0000 UTC 1 May of Sawyer-Eliassen streamfunction (black contours, dashed contours represent negative values) every 300 m hPa s^{-1}, moisture flux due to the Sawyer-Eliassen circulation every -3 cm s^{-1} beginning at 0 cm s^{-1} (0 cm s^{-1} is contoured in orange with the orange fill pattern used for values less than -3 cm s^{-1}), and negative omega associated with the Sawyer-Eliassen circulation every 1 dPa s^{-1} (blue fill pattern, dashed contours) beginning at 1 dPa s^{-1}. The sense of the circulation is denoted by the arrowheads plotted on the streamfunction contours and the location of the polar jet core is indicated by the "J".

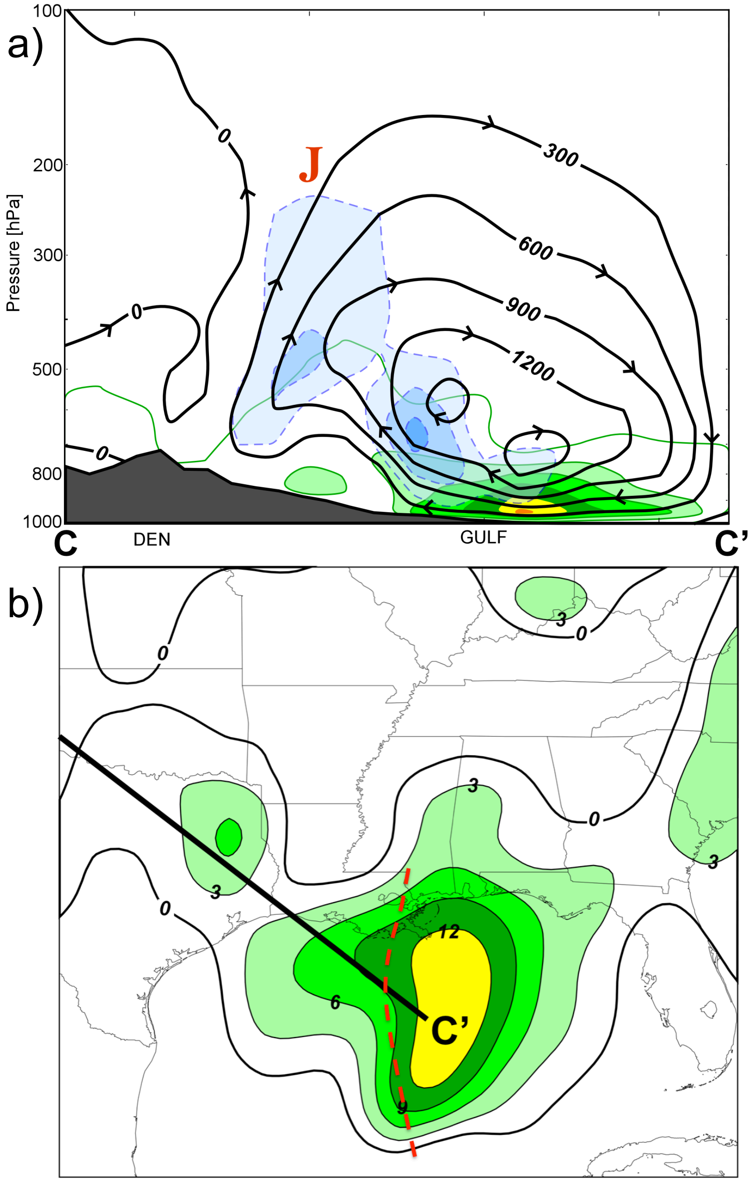

FIG. 12. (a) Cross section of Sawyer-Eliassen streamfunction along the line C-C', in Fig. 7b, at 0000 UTC 2 May. Labeling conventions are identical to those in Fig. 10a, with the "J" representing the superposed jet core. (b) As in Fig. 10b but valid at 0000 UTC 2 May.

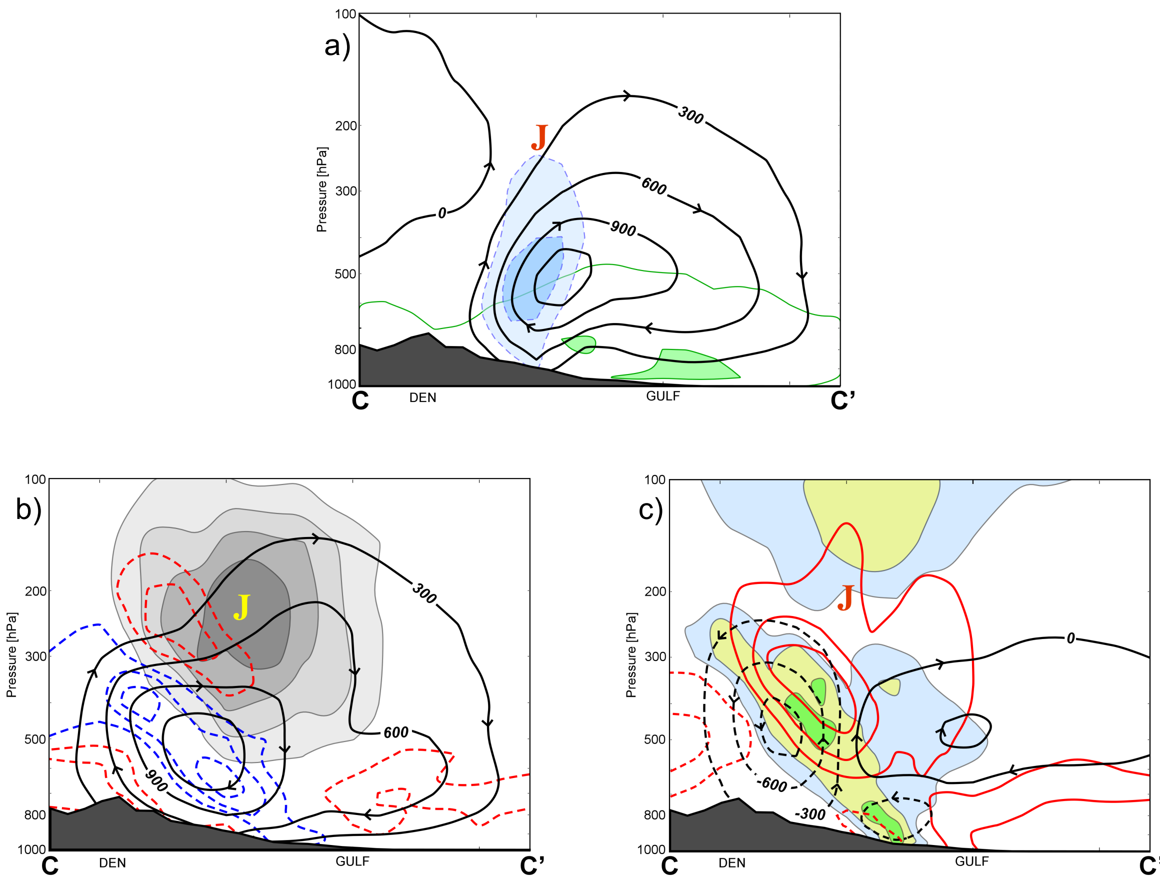

FIG. 13. Cross section along C-C', in Fig. 7b, at 0000 UTC 2 May showing: (a) the Sawyer-Eliassen streamfunction, poleward moisture flux, and negative omega (same conventions as Fig. 10a) associated with the Q_g forcing, (b) the Sawyer-Eliassen streamfunction associated with the Q_{SH} forcing (same conventions as Fig. 11), isotachs of the cross-section normal geostrophic wind (gray fill pattern) every 10 m s^{-1} beginning at 30 m s^{-1}, and the cross-section normal temperature gradient (negative, red dashed contours; positive, blue dashed contours) every 5×10^{-6} K m^{-1} (zero line omitted), (c) the Sawyer-Eliassen streamfunction associated with the Q_{ST} forcing (same conventions as Fig. 11), isotachs of the along-cross section geostrophic wind with positive values oriented towards C (positive, thick red lines; negative, dashed red lines) every 5 m s^{-1} (zero line omitted), and magnitude of the along-cross section potential temperature gradient every 10×10^{-6} K m^{-1} beginning at 10×10^{-6} K m^{-1} (fill pattern). The "J" represents the location of the superposed jet core in all panels.

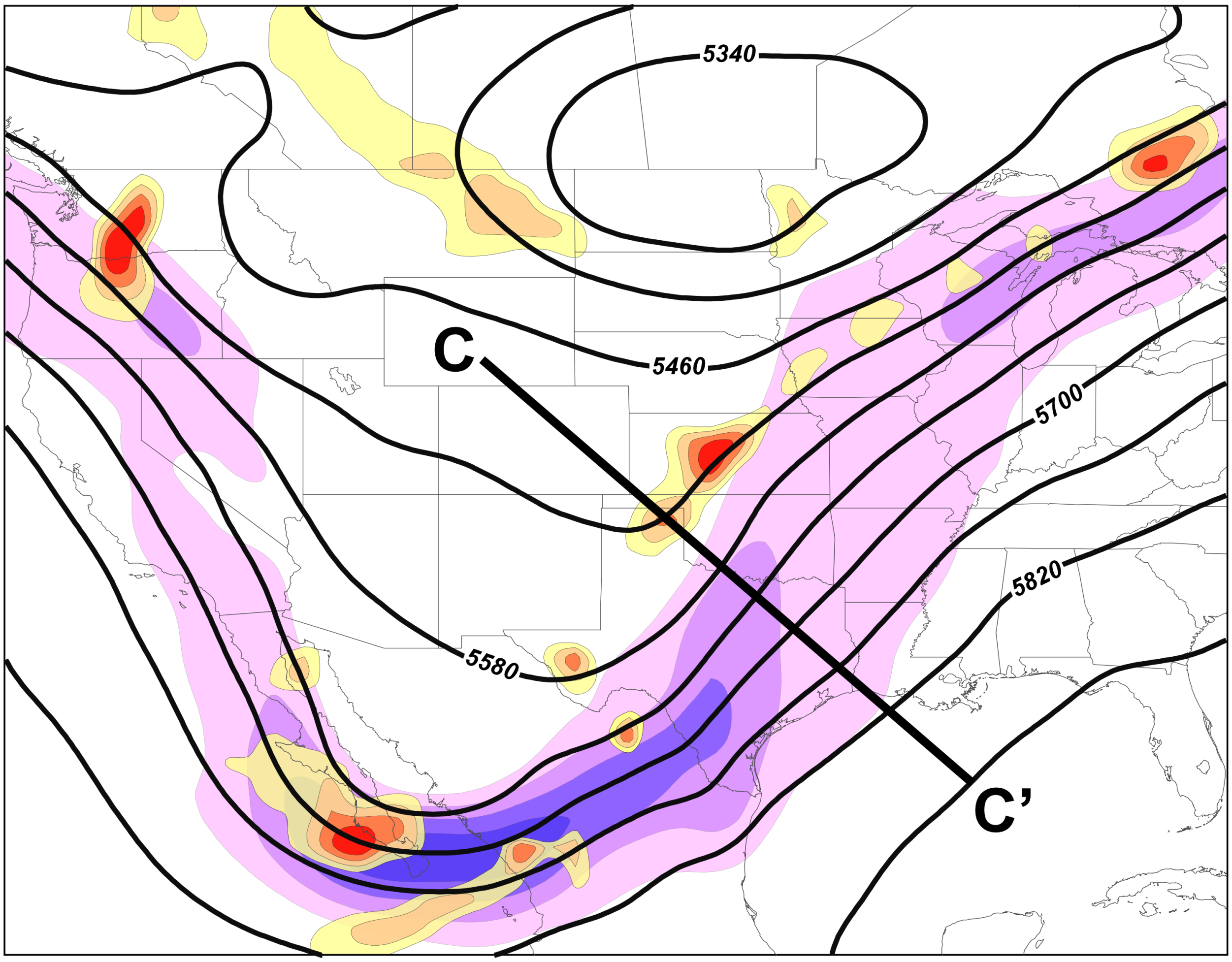

Fig. 14. 500 hPa GFS analysis at 0000 UTC 2 May with geopotential height contoured in black every 60 m, isotachs of the geostrophic wind (purple fill pattern) every 10 m s^{-1} beginning at 30 m s^{-1}, and horizontal geostrophic frontogenesis (warm colored fill pattern) every 0.4 K (100 km)$^{-1}$ (3 h)$^{-1}$ beginning at 0.4 K (100 km)$^{-1}$ (3 h)$^{-1}$.

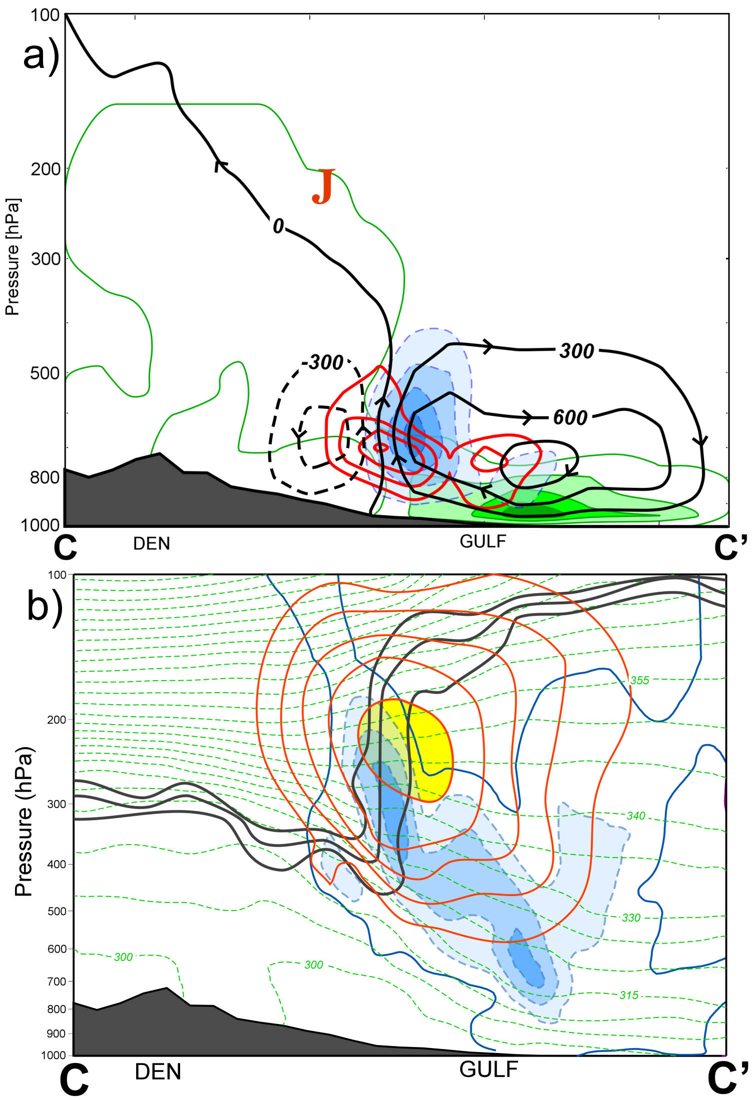

FIG. 15. (a) Sawyer-Eliassen streamfunction, poleward moisture flux, and negative omega, labeled, contoured, and shaded as in Fig. 10a, associated with the diabatic forcing. Heating labeled in K s^{-1} and contoured every 200×10^{-6} K s^{-1} beginning at 200×10^{-6} K s^{-1} (red contours). The "J" denotes the location of the superposed jet core. (b) 300 hPa isotachs (red contours) every 10 m s^{-1} beginning at 30 m s^{-1} with the jet core shaded yellow, 1,2,3 PVU surfaces (black contours), potential temperature every 5K (dashed green contours), and negative omega every 2 dPa s^{-1} beginning at 0 dPa s^{-1} (0 dPa s^{-1} is contoured in blue with values greater than 2 dPa s^{-1} shaded with the blue fill pattern) from the GFS analysis at 0000 UTC 2 May 2010 along the cross section C-C', in Fig. 7b.

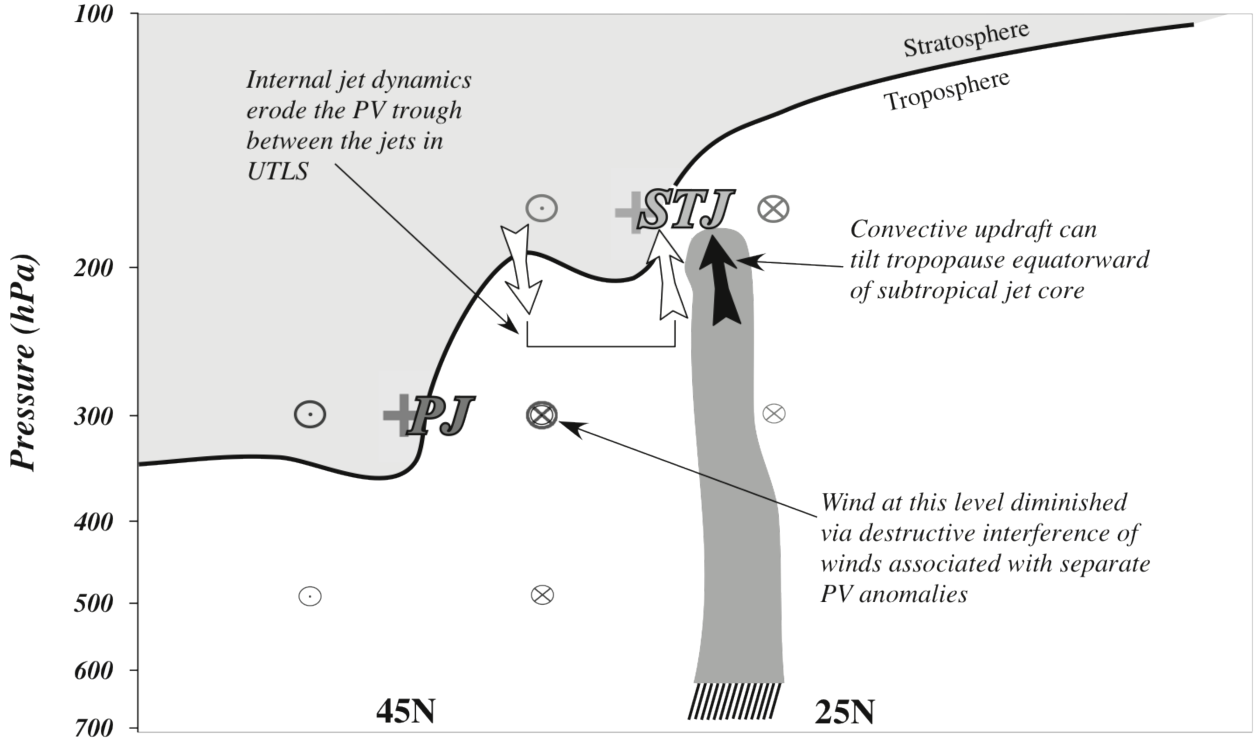

FIG. 16. Schematic vertical cross section illustrating the dynamical processes that may facilitate a superposition of the polar (PJ) and subtropical (STJ) jet. Each jet is associated with a tropopause level positive PV perturbation (signified by the + signs). Corresponding circulations at and below each perturbation are indicated by a circled × or •. Solid black line is the 1.5 PVU isosurface with the lower stratosphere shaded gray. See text for additional explanation.